UNIVERSITY OF NIŠ

ISSN 0354-804X (Print)
ISSN 2406-0534 (Online)
COBISS.SR-ID 72210956
UDC 502/504

FACTA UNIVERSITATIS

Series
WORKING AND LIVING ENVIRONMENTAL PROTECTION

Vol. 21, N° 2, 2024

Scientific Journal **FACTA UNIVERSITATIS**
UNIVERSITY OF NIŠ
Univerzitetski trg 2, 18000 Niš, Republic of Serbia
Phone: +381 18 257 095 Telefax: +381 18 257 950
e-mail: facta@ni.ac.rs http://casopisi.junis.ni.ac.rs/

Scientific Journal FACTA UNIVERSITATIS publishes original high scientific level works in the fields classified accordingly into the following periodical and independent series:

Architecture and Civil Engineering
Automatic Control and Robotics
Economics and Organization
Electronics and Energetics
Law and Politics
Linguistics and Literature
Mathematics and Informatics
Mechanical Engineering
Medicine and Biology
Philosophy, Sociology, Psychology and History
Physical Education and Sport
Physics, Chemistry and Technology
Teaching, Learning and Teacher Education
Visual Arts and Music
Working and Living Environmental Protection

SERIES **WORKING AND LIVING ENVIRONMENTAL PROTECTION**

Publication frequency – one volume, three issues per year.
Published by the University of Niš, Republic of Serbia

Printed by ATLANTIS DOO, Niš, Republic of Serbia
Circulation 50

ISSN 0354 – 804X (Print)
ISSN 2406 – 0534 (Online)
COBISS.SR-ID 72210956
UDC 502/504

FACTA UNIVERSITATIS

SERIES **WORKING AND LIVING ENVIRONMENTAL PROTECTION**

Vol. 21, Nº 2, 2024

UNIVERSITY OF NIŠ

INSTRUCTIONS FOR CONTRIBUTORS

Contributions should be (preferably) in English, French or German.
Under the paper title, the name(s) of the author(s) should be given while the full name, official title, institute or company affiliation and the like should be placed at the end of the paper together with the exact mail and e-mail address, as well as short (running) title of paper.
Manuscript format. A brief abstract of approximately 100 to 150 words in the same language and a list of up to six key words should precede the text body of the manuscript. All the authors apart from foreign ones should also submit a complete manuscript in Serbian. Manuscript should be prepared using a Word template, downloaded from web address:
http://casopisi.junis.ni.ac.rs/index.php/FUWorkLivEnvProt/about/submissions#authorGuidelines
Manuscript length. Brief articles and discussions (10 pages or less) are encouraged. Otherwise, papers should present well-focused arguments of approximately 16 pages.
Style requirements. **Letters, figures and symbols** should be clearly denoted.
Equations should be typewritten and, with the number, placed in parentheses at the right margin. References to equations should be in the form "Eq. (2)" or simply (2). For equations that cannot be entered in a single line, use the Equation Editor in MS Word. In equations and in the text, *italicize* symbols that are used to represent variables or parameters, including subscripts and superscripts. Only use characters and symbols that are available in the Equation Editor, in the *Symbol font* or in *Times New Roman*.
All illustrations (figures, photographs, line drawings, graphs) should be numbered in series and all legends should be included at the bottom of each illustration. All figures, photographs, line drawings and graphs, should be prepared in electronic form and converted in TIFF or JPG (max quality) file types, in 300 dpi resolution, for superior reproduction. Figures, line drawings and graphs prepared using elements of MS Drawing or MS Graph must be converted in form of pictures and unchangeable. All illustrations should be planned in advance so as to allow reduction to 12.75 cm in column width. Please review all illustrations to ensure that they are readable.
All **tables** should be numbered with consecutive Arabic numbers. They should have descriptive captions at the top of each table and should be mentioned in the text.
References should be listed alphabetically at the end of the manuscript, in the same way as the following examples (for a paper in a journal, a book, paper in a contributed volume and for an unpublished paper):

1. Connor, J. J., Logcher, R. D. and Shing-Ching, C.: *Nonlinear Analysis of Elastic Framed Structures*, J. Struct. Div., ASCE Vol. **ST** 6, pp. 1525-1547, 1968.
2. Arriaga F. and others: *Grading and load carrying capacity determination of old timber beams*, American Society for Agricultural Engineers, paper No 92-4068, 1992.
3. J. N. Reddy: *A refined nonlinear theory of plates with transverse shear deformation*, J. Solids and Struct., Vol bf 20, pp. 881-896, 1984, Comput. Struct., Vol. **5**, pp. 257-260, 1975.

References should be quoted in the text by the corresponding number in square brackets.

Electronic submission. Papers for consideration should be submitted to the Series Editor in electronic form via the Journal's home page: http://casopisi.junis.ni.ac.rs/index.php/FUWorkLivEnvProt.

FACTA UNIVERSITATIS

Series

Working and Living Environmental Protection

Vol. 21, Nº 2, 2024

Contents

FACTA UNIVERSITATIS
Series: **Working and Living Environmental Protection** Vol. 21, Nº 2, 2024, pp. 77 - 86
https://doi.org/10.22190/FUWLEP240410007M

Original Scientific Paper

PERFORMANCE ASSESSMENT OF SOLAR THERMAL HEAT STORAGE

UDC 620.91:536.24

Milena Mančić[1], Miomir Raos[1], Milena Medenica[1], Milan Protić[1], Marjan Popović[2], Marko Mančić[3]

[1]University of Niš, Faculty of Occupational Safety in Niš, Serbia
[2]MipHem, Belgrade, Serbia
[3]University of Niš, Faculty of Mechanical Engineering, Serbia

ORCID iDs:		
	Milena Mančić	https://orcid.org/0000-0002-6181-2286
	Miomir Raos	https://orcid.org/0000-0001-5586-0276
	Milena Medenica	https://orcid.org/0000-0001-6561-5696
	Milan Protić	https://orcid.org/0000-0003-4957-7882
	Marjan Popović	N/A
	Marko Mančić	https://orcid.org/0000-0001-7078-9658

Abstract. *Over the past thirty years, there has been a notable increase in electricity usage within the residential sector of Europe. Final energy consumption in the EU residential sector has risen by 26.3%, with heating systems/electric boilers accounting for a substantial portion at 19.1% of final energy usage. Additionally, the combined utilization of solar energy for heating and cooling presents an opportunity to elevate solar thermal energy from primarily providing domestic hot water to becoming a major energy source for buildings, complete with hot water storage buffers. This study presents a model of a solar thermal system with heat storage, simulated using TRNSYS software, based on typical meteorological conditions in Nis, Serbia. The system is designed for heating domestic hot water, and scenario analysis is conducted to assess the advantages of solar thermal applications compared to electric hot water heaters. The findings suggest significant savings in electricity usage and costs are possible, although careful consideration is needed when sizing solar thermal systems to prevent stagnation during the summer months.*

Key words: *heat storage, solar thermal, household energy balance*

Received April 10, 2024 / Accepted October 11, 2024
Corresponding author: Milena Mančić
Faculty of Occupational Safety, Univesity of Niš, Čarnojevića 10a, 18000 Niš, Serbia
E-mail: milena.mancic@znrfak.ni.ac.rs

1. Introduction

Over the last three decades, the electricity consumption of the residential sector in the European Union (EU-27) showed a great increment from 1990 to 2005 [1], and from 2005 to 2019 it is either in stagnation or its increase is minor; however, the residential sector is still the second biggest in electricity consumption, right after industry. Households use energy for various purposes: space and water heating, space cooling, cooking, lighting and electrical appliances, and other end-users (mainly covering uses of energy by households outside the dwellings themselves). Data on the energy consumption of households broken down by end-use, have been collected and published by Eurostat since 2017. In 2019, households, or the residential sector, represented 26.3 % of final energy consumption or 16.9 % of gross inland energy consumption in the EU [2]. During the 10-year period from 2009 to 2019, the consumption of electricity by households in the EU rose by 0.8 %. These figures on overall household electricity consumption are likely to be influenced, in part, by the average number of people living in each household and by the total number of households, both of which are linked to demographic events. Other influences include the extent of ownership and use of electrical household appliances and consumer goods as well as the use of energy-saving devices [2]. Furthermore, energy consumption for heating and cooling of a household is strongly affected by the level of energy efficiency measures implemented in the household (thermal insulation, quality of glazing, applied heating and cooling energy transformation technologies, etc.), whereas the electricity consumption is also affected by the energy efficiency rating of the household appliances.

The residential sector is the second most important final energy "consumer" with almost 30% of the total electricity consumption. This is the main reason why the efficient use of energy by domestic appliances, along with the possibility of recovering and reusing their waste heat, is becoming more and more relevant.

1.1. Energy consumption in households in Europe and Serbia

The energy consumption of households in the EU decreased between 2005 and 2016 [8,9]. During the last 15 years, energy efficiency improvements in space heating and the use of more efficient electrical appliances, as well as behavioral changes driven by higher energy prices and the 2008 economic downturn all contributed to reductions in overall energy consumption in the household sector. Increases in the number of appliances, average size of dwellings, and number of dwellings partially offset these improvements [8].

Household energy consumption increased both in 2015 (by 4 %) and in 2016 (by 3 %) compared with 2014 and 2015 respectively. The relatively colder winters in these two years contributed to these increases. However, lifestyle changes such as more dwellings, more appliances per dwelling, and changes in heating behavior (e.g. higher indoor temperatures) also contributed. Energy efficiency improvements were not significant enough to counteract these effects. In fact, since 2013 a slowdown in the rate of the annual energy efficiency improvement has been observed year-on-year compared with the average annual rate of the 2005-2016 period. [8-11]

Energy use in the household sector differs widely between countries because of weather conditions, the state and age of the building stock and household appliances, the average size of the dwellings, the heating/cooling systems used, behavior (particularly with respect to cooking) and the level of implementation of energy efficiency measures. In 2016, per capita energy consumption in the household sector of the EU countries ranged from 0.2 tons of oil equivalent per capita (toe/capita) in Malta to 1 ton/capita in Finland [2, 8-11].

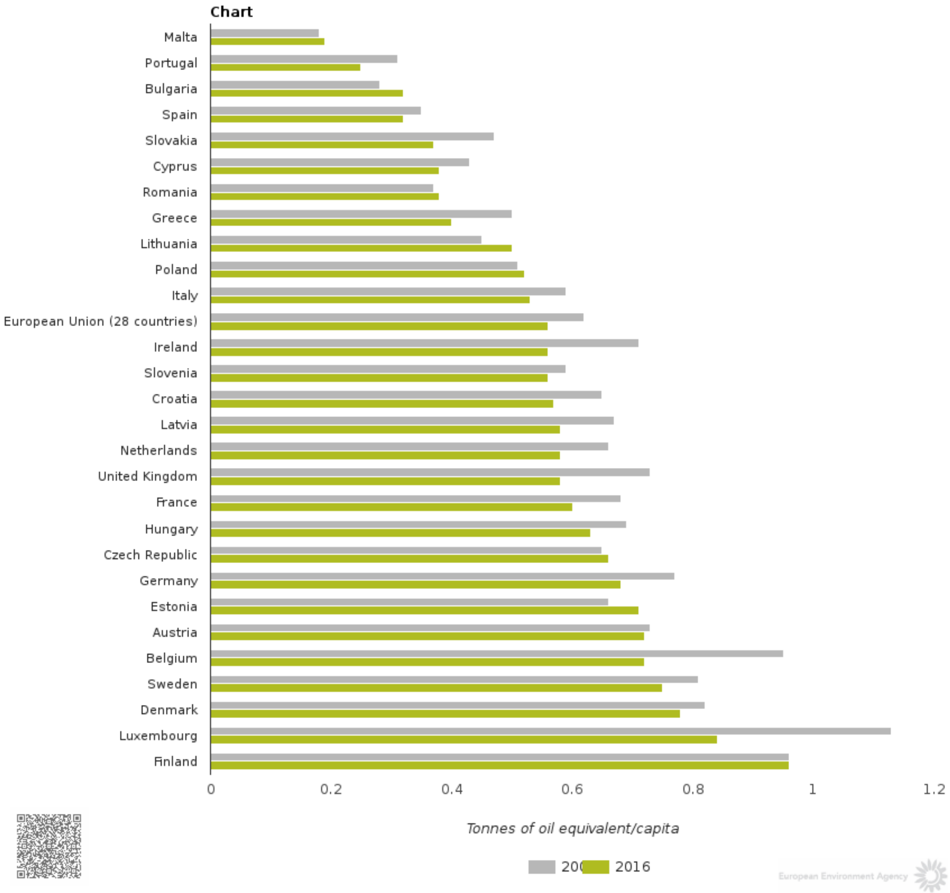

Fig. 1 Per capita final energy consumption of the household's sector, by country

As you can see in Figure 1. [8-11], the biggest consumer in Europe, from all 27 countries is Finland, and right next to Finland are Luxembourg, Denmark, Sweden. The explanation can be found in climate and temperature in the wintertime in those countries. For comparison, Finland used 67.46 TWh of electricity in 2020, while Serbia used 35.52 TWh. Like total energy consumption, the amount of electricity a country consumes in total is largely reflected by population size, as well as the average incomes of people in the given country.

There is a tendency for increased energy consumption in Serbia, while total dependency on imported energy, mostly petroleum and its products, is around 40% [4]. The housing industry's share in energy consumption amounts to 48% of total consumption, 65% of which refers to energy consumption in residential buildings ranging from 150 to 250 kWh/m2 on average [3]. [16]

1.2. Common appliances in households and their consumption

According to literature, the number of domestic appliances in the European Union is continuously growing and the same goes for how often that appliance is in use, as well as for the duration of their duty cycles. That is the reason why despite the continuous development of high-efficiency appliances, it is expected that electricity consumption in the residential sector continuously increases. Heating systems/electric boilers represent the highest share, about 19.1%, of the residential electricity consumption at the European level [1]. While the second, third and fourth place is reserved for refrigerators and freezers with energy consumption of almost 14.5%, then electric ovens, washing machines/dryers and dishwashers contribute to the electricity consumption of 6.6%, 7.2% and 3% respectively [12]. The European Union is required to meet standards that imply eco-responsiveness and information for the design of efficient household appliances. Based on the higher performances of the new appliances, in July 2011, new labelling directives were adopted introducing new energy efficiency classes (A+++, A++ and A+) to the already available (A-G). In addition, considering the most recent data available regarding [1,12-14] the performance and diffusion of household appliances, an assessment of the waste heat produced was carried out with the aim of evaluating the amount of thermal energy which should potentially be recovered and reused. At the European level, the most common household appliances are given in Table 1.

Table 1 Energy consumption analysis for appliances that are the biggest consumers

Appliance	Average energy consumption [kWh/cycle]	Temperature [ºC]
Refrigerators and freezers	640Wh/24h	35-50
Electric ovens	1.25	35-250
Dichwashers	0.8-0.95	40
Washing machines	1	30-35

According to the model given in the literature, parameters of active and stand-by consumption of an appliance are linked to the annual consumption model according to the following equation [3,6]:

$$E_{yearly} = \left(3600 \times 24 \frac{s}{day} \dot{E}_{stand-by} + f \sum_{n=1}^{n_{cycle}} \dot{E}_{cycle,n} \, t_{cycle} \right) \frac{365}{3,6 \times 10^6} \frac{daykWh}{W\,s} \tag{1}$$

where E_{yearly} is the mean consumption (kWh), $E_{stand\text{-}by}$ is the electric load of an appliance in stand-by, $E_{cycle,n}$ is the electric load during a mean consumption cycle (W), t_{cycle} is time step in the duration of a mean consumption cycle (s), and n_{cycle} is the number of time steps of the mean consumption cycle. The difference in behavior profile-electrical load on the typical working day and at the weekend was considered negligible. Basic energy-efficient rated appliances were included in the model: Television, electrical stove, Compact Disc player, personal computer, refrigerator with freezer, microwave oven, washing machine, and dishwasher. Thermal gain from the use of these appliances was included in the thermal balance of the building. The trend of change in daily electricity consumption due to climate changes throughout the year was synchronized with data from 41 by multiplying the time step value of electrical load by a monthly weight factor of the corresponding time interval [3,6,7].

1.3. Thermal storage and its function

Heat storage, also known as thermal energy storage (TES), generally involves the temporary storage of high- or low-temperature thermal energy for later use [15]. Heat storage

(HS) stores thermal energy for later use. TS systems are used in buildings and industrial heating/cooling applications, but in recent years it has become very common that even the residential sector increasingly uses heat storage. TES systems reduce peak demand, energy consumption, CO2 emissions, and costs. In literature, TES is described as “an advanced energy technology that is attracting increasing interest for thermal applications such as space and water heating, cooling, and air conditioning.”

Examples of heat storage applications include storage of solar energy for overnight heating, storing summer heat for winter use, winter ice for space cooling in summer, and storing electrically generated heat or cool power during off-peak hours for use during subsequent peak demand hours. In this regard, a heat storage system is in many instances a useful device for offsetting temporal mismatches between thermal energy availability and demand.

All heat storage systems have three functions:

1. Charge: a heat source is used to provide heat to the storage medium.
2. Storage: a medium is used to store the heat for later use. The storage medium may be located at the heat source, the discharge, or somewhere else.
3. Discharge: heat is extracted from the storage medium in a controlled fashion for use.

In addition, all heat storage systems have three basic components: a control system that makes it easier to charge and discharge the thermal storage, a heat exchanger to help transfer heat to and from the storage material, and storage material and, if applicable, a container for the storage material.

1.4. Optimal capacity of thermal storage

The combined use of solar energy for heating and cooling has the potential to upgrade solar thermal energy from a major DHW provider to a major building energy supplier. The simulation of the system is done in Trnsys software, and the scheme is given in Figure 2. A closed loop consisting of an evacuated tube solar collector and a variable speed pump provides the hot stream of a heat exchanger within a sealed tank filled with an energy storage medium such as non-potable water. Water is drawn from the mains through another heat exchanger within the same tank and preheated before delivery to the storage tank, where it is further heated by gas (if necessary) before use.

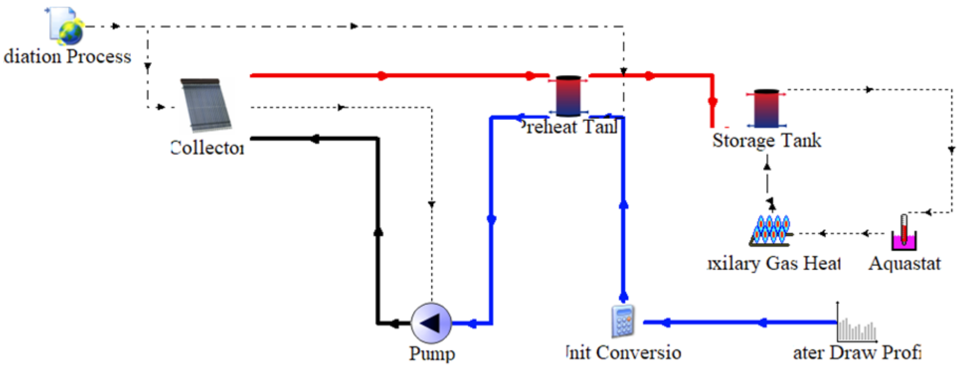

Fig. 2 Schematic representation of the considered system

As it is given in Figure 2, we have two solar collectors, one Preheat storage tank and one Storage tank. The solar collectors are chosen to respond to demands so that the system does not enter the realm of stagnation, and it is the reason why we have a reheater (also presented in Figure 2).

The components that we used in our simulation are:

1. Radiation Processor- provides solar radiation data, ambient temperature, and water mains temperature;
2. Collector -models evacuated tube solar collector; variable behavior;
3. Pump- Variable speed pump, controlled by collector behavior;
4. Preheat Tank- sealed tank with dual heat exchangers to provide preheating of mains water 0.5 m3;
5. Water Draw Profile - instant water draw profile used by SRCC;
6. Unit Conversion - converts from GPM to kg/hr;
7. Storage Tank- stores preheated water 1 m3;
8. Auxiliary heater - heats water in storage tank if necessary;
9. Aquastat -generates a control signal for the gas heater based on storage tank temperature.

2. RESULTS AND DISCUSSION

The results obtained by simulation are presented in the next few figures. The first simulation is given for the whole year, 8760h. The heat exchanger fluid is water with a density of 1000[kg/m3], thermal conductivity of 2.14 [kJ/hmK], and specific heat of 4.19 [kJ/kg K]. Tank properties are: number of tank nodes is 8, the tank volume is 1[m3], top and bottom loss coefficient is 5[kJ/hm2K], and initial tank node temperature is 55[ºC]. Solar collector has an array area of 2[m2], the number of nodes is 10, and the flow rate per unit area is 50[kg/hm2]. Aquastat is set so that fluid inlet temp. is 20[ºC], and setpoint temperature for stage is 50[ºC]. Hysteresis +/- 2 [ºC]. Preheater has a heating capacity of 16200[kJ/h]. The results in the paper are presented for a typical meteorological year, for the solar radiation data for Nis, Serbia, with 1h timestep resolution.

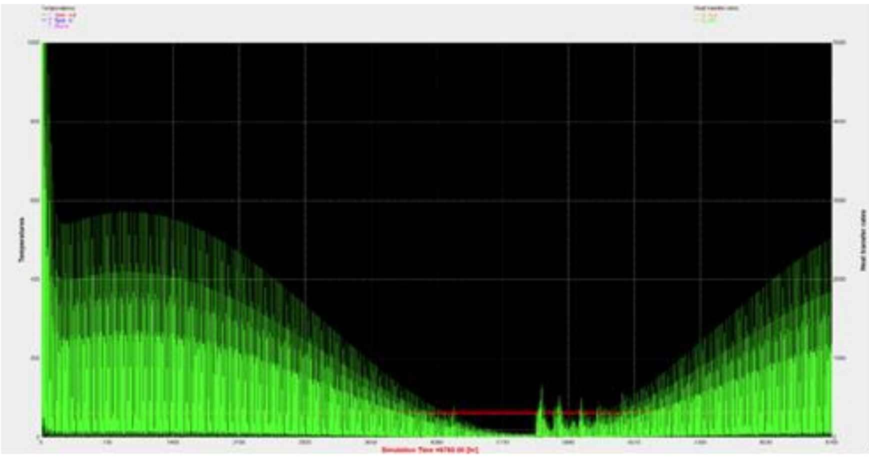

Fig. 3 Annual solar thermal system results (green – heat exchanger transferred energy in kJ/h, red – tank outlet temperature in ºC, blue Tank inlet temperature in ºC, purple – mains water temperature in ºC) ¶

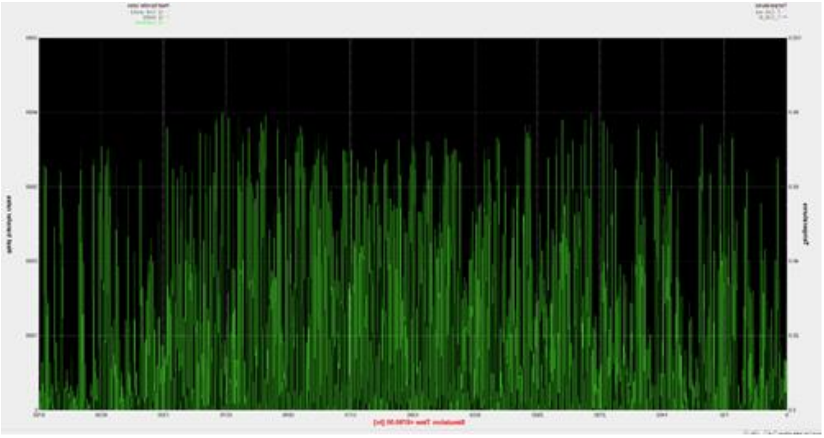

Fig. 4 The amount of the amount of solar radiation in kJ/h

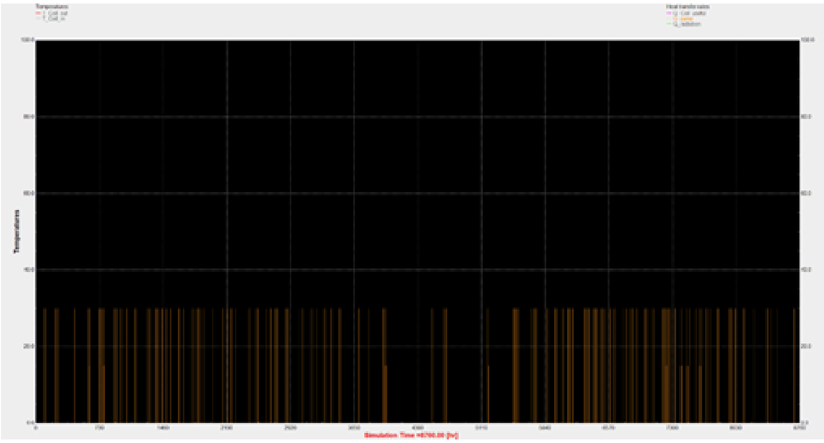

Fig. 5 Electricity used by the pump of the solar system in kJ/h

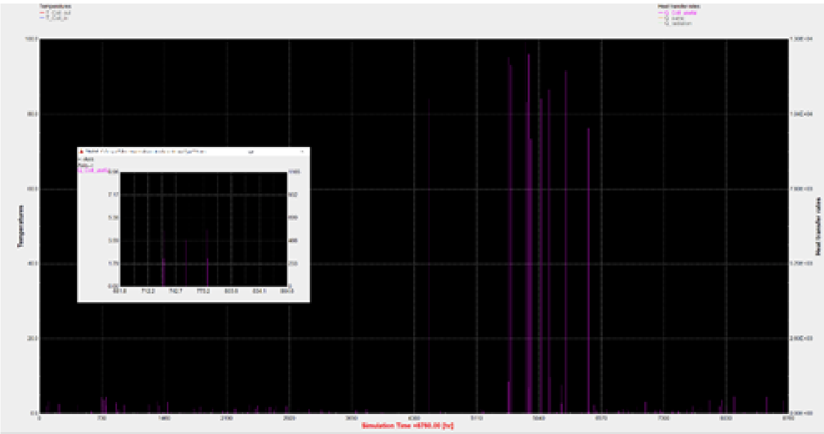

Fig. 6 Useful heat exchange from solar collector

In the first part of the year (first six months) and in the last three months of the year, the amount of useful heat given through solar collectors is much smaller than in July, August, and September. The explanation is simple – those are the winter, fall and early spring months. Furthermore, the utilization of the solar system is also dependent on the control system and the use of heat by the heat exchanger. Hence since the initial temperature of the tank is relatively high (55ºC), the water is heated using the heater, since the solar radiation is insufficient. In the summer period, the solar radiation is sufficient for the assumed consumption load, however, in the rest of the year it is utilized only when the temperature conditions are such, that the temperature is low enough to utilize solar energy, and the temperature in the solar collector in the same timestep is high enough for heating the tank(s). If this condition is not met, the tanks are heated by the heat exchanger-heater, resulting in poor effectiveness of the solar system, except in the hot summer munts. In the figure, you can see zoomed results for the January period.

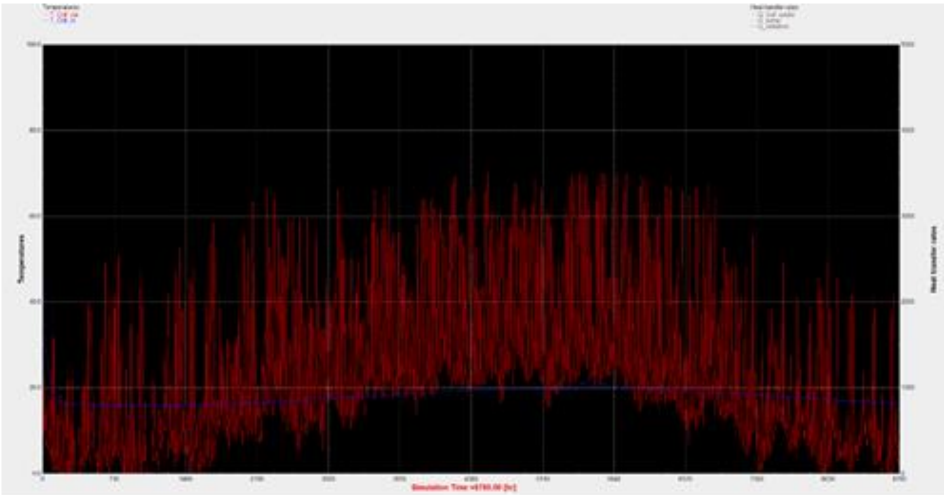

Fig. 7. Temperature inlet and outlet for Solar collector

As shown in Figure 7, the inlet temperature is practically the same throughout the year, no matter what time of day or year is, and as can be seen in Figure 7 that is not the case for outlet temperature. The inlet temperature is around 20 [ºC], with small fluctuation in the first three months of the year, and outlet temperature varies through the day, while at night it is lower, which depends on the time of the year. The highest outlet temperature is from May till September, and it can go to 73[ºC].

3. CONCLUSION

This paper presents and analyses the current state of energy consumption in households in the European Union. It is concluded that sanitary hot water accounts for almost 20% of household electricity consumption. An annual simulation of the solar evacuated tube collector system with an auxiliary heater is made for a typical meteorological year in Serbia. The simulation indicated that the design of the system and choice of hot water tank desired temperature level, as well as dynamics of the consumption and availability of solar energy can strongly affect the effectiveness of the solar system. As the simulation results show, if the hot water tank temperature is set too high, solar collectors may provide insufficient heat flux for most of the year, except for the summer period. The solar systems are sized this way, i.e. based on the minimum heat demand in the hottest summer periods, to avoid the so-called solar thermal system stagnation, which can lead to system damage. Therefore, for the high desired tank temperatures, the auxiliary heater is responsible for meeting most of the hot water energy demands. Different scenarios can be expected in the case of lower desired tank temperatures, but this can be analyzed in some future research and is omitted from this study.

Acknowledgement: *The paper is a part of the research done within the project NATO Science for Peace Multi-Year Project G6006, Acoustic Multi-Functional Composites for Environmental Risks and Health Hazards Reduction.*

REFERENCES

1. Simone A. Zavattoni, Nelson Garcia-Polanco, Joaquin Capablo, John P. Doyle, Maurizio C. Barbato, „Household Appliances Wasted Heat Storage by means of a Packed bed TES with Encapsulated PCM“, 13th International Conference on Sustainable Energy technologies (SET2014) 25-28th August, 2014 Geneva
2. Eurostat, Energy consumption and use by households
3. Goran Jovanovic, Dragoljub Živkovic, Marko Mančić, Vladana Stanković, Danica Stanković „A model of a Serbian energy efficient house for decentralized electricity production“, Journal of Renewable and Sustainable Energy 5, 041810 (2013); doi: 10.1063/1.4812997
4. M. Golusin, O. M. Ivanovic, I. Bagaric, and S. Vranjes, "Exploitation of geothermal energy as a priority of sustainable energetic development in Serbia," Renewable Sustainable Energy Rev. 14, 868 (2010).
5. Official Gazette of Republic of Serbia, No. 72/09, Ministry of Minings and Energy, Government of the Republic of Serbia, Belgrade, 2004.
6. J. V. Paatero and P. D. Lund, "A model for generating household electricity load profiles," Int. J. Energy Res. 30, 273 (2006).
7. S. Jovanovic, Z. Djordjevic, M. Bojic, S. Savic, and B. Stepanovic, "Weather conditions impact on electricity consumption," in Proceedings Conference on Mechanical Engineering Technologies and Applications COMETA 2012, Jahorina, Republic of Srpska, 28-30 November 2012, pp. 409–415.
8. EEA, 2018c, forthcoming, 'Progress on energy efficiency in Europe (ENER 037)' (https://www.eea.europa.eu/data-and-maps/indicators/progress-on-energy-efficiency-in-europe-2/assessment-2) European Environment Agency.
9. EC, 2016, Communication from the Commission to the European Parliament, the Council, the European Economic and Social Committee and the Committee of the Regions 'An EU strategy on heating and cooling' (COM(2016) 51 final) (https://ec.europa.eu/energy/sites/ener/files/documents/1_EN_ACT_part1_v14.pdf) accessed 14 February 2018.
10. EEA, 2018a, forthcoming, 'Final energy consumption by sector and fuel (CSI 027/ENER 016)' (https://www.eea.europa.eu/data-and-maps/indicators/final-energy-consumption-by-sector-9/assessment-1) European Environment Agency.
11. JRC, 2016, Energy consumption and energy efficiency trends in the EU-28 2000–2014 (http://publications.jrc.ec.europa.eu/repository/bitstream/JRC101177/ldna27972enn.pdf) accessed 14 February 2018.
12. Bertoldi, P., Hirl, B. & Labanca, N., 2012. "Energy efficiency Status Report 2012", s.l.: JRC - Joint Research Centre.
13. Programme, M. -. M. T., 2007. "BNC11: Domestic refrigerator test standard vs real-use energy consumption", s.l.: s.n.
14. Programme, M. -. M. T., 2008. "BNCK01: Assumptions underlying the energy projections of cooking appliances", s.l.: s.n

15. Marko Mančić, Dragoljub Živković, Pedja Milosavljevic, Milena Todorovic „Mathematical modelling and simulation of the thermal performance of a solar heated indoor swimming pool", THERMAL SCIENCE: Year 2014, Vol. 18, No. 3, pp. 999-1010
16. https://www.eea.europa.eu/data-and-maps/daviz/final-energy-consumption-households-per-capita-2#tab-chart_1.

PROCENA RADNIH KARAKTERISTIKA SOLARNOG AKUMULATORA TOPLOTE

Tokom proteklih trideset godina, došlo je do značajnog povećanja potrošnje električne energije u stambenom sektoru Evrope. Finalna potrošnja energije u stambenom sektoru EU porasla je za 26,3%, pri čemu sistemi grejanja/električni kotlovi čine značajan deo od 19,1% finalne potrošnje energije. Kombinovano korišćenje solarne energije za grejanje i hlađenje predstavlja priliku da se solarna toplotna energija podigne sa primarnog snabdevanja tople vode za domaćinstvo do toga da postane glavni izvor energije za zgrade, zajedno sa baferima za skladištenje tople vode. Ova studija predstavlja model solarnog termalnog sistema sa akumulacijom toplote, simuliran korišćenjem softvera TRNSIS, zasnovan na tipičnim meteorološkim uslovima u Nišu, Srbija. Sistem je dizajniran za zagrevanje sanitarne tople vode, a analiza scenarija je sprovedena kako bi se procenile prednosti solarne primene u poređenju sa električnim grejačima tople vode. Rezultati ukazuju na to da su moguće značajne uštede u korišćenju električne energije i troškovima, iako je potrebno pažljivo razmatranje kada se dimennzioniše ovakav sistem kako bi se sprečila stagnacija tokom letnjih meseci.

Ključne reči: *akumulatori toplote, solarni sistemi, toplotni bilans za objekte u rezidencijalnom sektoru*

FACTA UNIVERSITATIS
Series: **Working and Living Environmental Protection** Vol. 21, Nº 2, 2024, pp. 87 - 96
https://doi.org/10.22190/FUWLEP240605008V

Original Scientific Paper

SPATIAL DISTRIBUTION PATTERNS OF WILD-FIRES INCIDENTS IN SERBIA BASED ON VIIRS 375 M DATA FOR THE PERIOD 2013-2023

UDC 614.84:519.273.8(497.11)”2013/2023”

Petar Vranić[1], Nikola Mišić[2]

[1]Mathematical Institute of the Serbian Academy of Sciences and Arts, Belgrade, Serbia
[2]University of Niš, Faculty of Occupational Safety, Niš, Serbia

ORCID iDs: Petar Vranić https://orcid.org/0000-0002-9671-992X
Nikola Mišić https://orcid.org/0000-0003-2314-4851

Abstract. *This research investigates the spatial distribution and clustering patterns of wildland fires in Serbia from January 2013 to December 2023 using data obtained from NASA's Fire Information for Resource Management System (FIRMS). A total of 69,179 fires are mapped using the Visible Infrared Imaging Radiometer Suite (VIIRS) 375 m thermal anomalies/active fire product, which offers improved spatial resolution and mapping capabilities. Spatial autocorrelation analysis, particularly Moran's I and Local Moran's I, is applied to assess the degree of clustering in the wildland fire incident dataset. Results indicate significant spatial patterns, highlighting critical areas for fire management and prevention. Municipalities such as Požarevac, Bogatić, Kikinda, Žitište, Sečanj, Šid, Irig, Ruma, and Stara Pazova, identified as HH clusters, should be prioritized for resource allocation. LH clusters, including Grocka, Beočin, and Velika Plana, need integration into regional strategies. Additionally, the persistent HL cluster in Kosjerić indicates an anomaly requiring focused intervention. These insights provide valuable information for targeted fire management strategies and highlight the importance of spatial analysis in understanding wildfire dynamics.*

Key words: *wildfire, spatial analysis, clustering patterns, Moran's I, Local Moran's I, Serbia*

1. INTRODUCTION

Climate change is responsible for the increased severity and frequency of natural disasters, including wildland fires, which significantly impact the environment, economy, and development of affected areas. The occurrence of wildland fires results from a complex interaction among ignition sources, weather, topography, and land cover [1]. The changes

Received June 5, 2024 / Accepted October 11, 2024
Corresponding author: Petar Vranić
Mathematical Institute of the Serbian Academy of Sciences and Arts, Kneza Mihaila 36, 11000 Belgrade, Serbia
E-mail: petarvvv@gmail.com

in land use, and land management significantly influence the occurrence and severity of wildland fires globally. This is especially noticeable in Europe, where shifts in land use have substantially altered fire patterns in recent decades. While the European Forest Fire Information System's satellite data offers extensive wildland fire statistics across European countries, there remains a critical need for detailed local analysis and a deeper understanding of the wildland fire conditions and associated challenges throughout Europe [2].

Projections indicate an increase in fire danger and burnt areas in southern Europe, with varying estimates of the increase per decade under high greenhouse gas emission scenarios [3]. This paper reviews 23 projection studies focusing on future wildland fire danger and activity in southern Europe, highlighting the increasing research effort on this topic. The review discusses the limitations and uncertainties in current wildland fire projections, including challenges related to climate projections, climate-fire models, and the influence of fuels, fire-vegetation feedbacks, and human-related factors on climate-fire relationships.

Using the standalone fire model (SFM), Khabarov et al. (2016) estimate a potential 200% increase in burned areas in Europe by 2090 under a 'no adaptation' scenario compared to 2000-2008, highlighting the urgency for effective adaptation measures. Under the same scenario, Balkan and Eastern European countries are projected to experience an extreme increase of 150-560% in burned areas by 2090 compared to 2000 [4].

In an attempt to address these challenges plethora of approaches are developed. To create a fire danger index for wildland fires, it is necessary to consider a wide range of factors beyond the weather forecast, such as fuel, moisture content, and topography. Due to the unavailability of information on the amount of combustible vegetative material, moisture content, and similar factors, leading world institutions such as Natural Resources Canada (NRC), the US National Oceanic and Atmospheric Administration (NOAA), and the Global Fire Early Warning System have implemented regional fire hazard forecasting systems based on their operational meteorological data, such as temperature, humidity, and precipitation, gathered from weather stations [5].

In addition to the previously mentioned models, geographical information systems (GIS) coupled with various methods proved to be suitable tools for fire danger mapping, fuel management, and fire effects assessment. For better visualization, several hazard variables such as vegetation type, topography, soil, and fire history can be additionally implemented in GIS applications [6]. On this subject, various authors have demonstrated the capacity of GIS to enhance the spatial analysis of fire danger indices, which are used for fire prevention and pre-suppression planning.

Gheshlaghi (2019) employed Geographic Information System (GIS) and Multi-Criteria Decision Analysis (MCDA) methods to produce forest fire risk maps [7]. The study utilized the GIS-based Analytical Network Process (ANP) as an MCDA method to create a fire risk map incorporating factors such as slope, altitude, land cover, and climate data. The results of this study included developing decision-making structures, calculating weighted supermatrices, and determining final priorities for accurate forest fire risk mapping.

The MODIS fire dataset, provided by The Fire Information for Resource Management System (FIRMS), offers access to satellite imagery, active fire/hotspots, and related products to identify the location, extent, and intensity of wildfire activity [8]. Levin and Heimowitz (2012) reviewed other databases, such as Landsat. However, they preferred to use the MODIS database because Landsat does not offer the temporal resolution and spatial coverage needed to monitor fires regularly and consistently. They quantified the spatial and temporal patterns of wildland fires in Israel since 2000 to analyze the physical and human factors leading to fire occurrence. By mapping wildland fire hotspots, it is possible to assess whether the fire risk is higher and to explain how land-cover and land-use patterns determine wildland fire risk [9].

Using data from the MODIS fire dataset and the receiver operating characteristic (ROC) method, Salma et al. (2023) validated the risk zones identified by the MCDA-AHP model and GIS [10]. They calculated the contribution of each factor, whether natural or anthropogenic, leading to fire initiation. The validation of the map confirmed the effectiveness of the employed model, providing a reliable tool for assessing wildfire risk zones.

Nikhil et al. (2021) highlight the importance of factors such as land cover types, slope angle, aspect, topographic wetness index, and distances from settlements, roads, tourist spots, and anti-poaching camp sheds are crucial for determining wildland fire risk zones. In the study, the application of GIS and the analytical hierarchy process (AHP) were employed to delineate forest fire susceptible zones, showcasing the utility of these approaches in fire risk assessment [11]. The research in [12] provides a comprehensive forest fire risk map using GIS-MCDA, AHP, and statistical analysis, aiding in proactive forest fire management.

By identifying and mapping Wildland-Urban Interface (WUI) areas based on building configuration and forest fragmentation, the study in [13] helps in understanding the spatial patterns of WUI and wildfire ignition points. The study highlights the vulnerability of peri-urban areas with dense clusters of buildings surrounded by forestland to fire ignition, emphasizing the need for targeted prevention strategies in such regions.

Nami et al. (2018) show the practical implications of integrating GIS-automated techniques with the quantitative data-driven evidential belief function (EBF) model for accurate estimation of wildfire probability. A wide range of predictor variables such as aspect, elevation, land use and land cover, soil type, and proximity to infrastructure were utilized, highlighting the importance of considering various factors in predicting fire occurrence. The study underscores the significance of human activities and infrastructure in influencing fire probability, suggesting the need for monitoring and managing these factors to mitigate wildfire risks effectively [154].

The research in [15] focused on predicting human-caused grassland fires using GIS spatial analysis and logistic regression, emphasizing the importance of assessing fire danger and weather conditions for fire management. The model developed in the study utilized topography, weather factors, and distances to human-built infrastructure to predict the probability of human-caused grassland fires. Correlations were found between ignition probabilities and various variables. The spatial distribution of ignition probabilities was higher in regions with greater human infrastructure density, such as villages and dirt roads, indicating a link between human activities and fire ignition.

Climate change in Serbia and the West Balkan region presents significant challenges, impacting various economic sectors and heightening the risk of natural disasters such as droughts, floods, and wildland fires. Notably, stubble burning poses a significant risk for wildland fires in Serbia, especially since these fires are more likely to spread from fields to forests.

A reliable network for monitoring wildland fires does not exist in Serbia, making it difficult to effectively manage and mitigate fire risk. The Emergency Management Sector of the Ministry of Internal Affairs of the Republic of Serbia maintains an internal database with general information on all fires where firefighter units operated. This database can provide the necessary input data for developing a unified network system for decision support to enable adequate forest fire risk management in wildland areas. By upgrading this database with diverse variables such as vegetation, topography, and distance from roads, rivers, and human settlements, this system would become a valuable tool for wildfire mitigation, offering real-time information, predictive analytics, and strategic guidance to improve preparedness and response efforts.

Due to inappropriate application and outdated legal directives regarding wildland fire protection, as well as a lack of appropriate infrastructure, insufficient human resources for fire prevention and suppression, and ineffective information distribution, there is a pressing need for a national decision-support system to effectively manage adaptation projects at both national and subnational levels [2,16].

In accordance with the Serbian Law on Fire Protection[1] the local self-government units (municipality), within the competence established by the Constitution and the law, organizes and ensures the conditions for the implementation of fire protection measures and the provision of assistance in eliminating or mitigating the consequences caused by fire and passes acts to improve the state of fire protection. The local self-government unit adopts the Fire Protection Plan, which includes, among other things, an assessment of the risk of fire.

The main objective of this research is to provide an in-depth understanding of the spatial distribution patterns of wildland fire incidents in Serbia over the period 2013-2023, specifically at the municipal level. By applying spatial autocorrelation (Moran's I and Local Moran's I), the research seeks to highlight critical areas for fire management and prevention, thereby offering valuable insights for targeted resource allocation and strategic interventions.

2. Methods and Data

2.1. Data

In this research data regarding fire incidents were obtained from NASA's Fire Information for Resource Management System (FIRMS). Specifically, the Visible Infrared Imaging Radiometer Suite (VIIRS) 375[2] m thermal anomalies / active fire product is used. This product complements Moderate Resolution Imaging Spectroradiometer (MODIS) fire detection, with the improved spatial resolution of the 375 m data that provides a greater response over fires of relatively small areas and provides improved mapping of large fire perimeters. The product uses a multi-spectral contextual algorithm to identify sub-pixel fire activity and other thermal anomalies.

For the period from January 2013 to December 2023, 69179 fires are mapped. For the analysis only fire pixels with nominal and high confidence are considered, 95% of a total number of fire pixels mapped. Nominal confidence pixels are those free of potential sun glint contamination during the day and marked by strong (>15K) temperature anomaly in either day or night-time data. High confidence fire pixels are associated with day or night-time saturated pixels.

---

[1] "Official Gazette of RS", no. 111/2009, 20/2015, 87/2018 and 87/2018 - other laws

[2] VIIRS 375m NRT (Suomi NPP) NRT VIIRS 375 m Active Fire product VNP14IMGT distributed from NASA FIRMS. Available on-line https://earthdata.nasa.gov/firms. doi:10.5067/FIRMS/VIIRS/VNP14IMGT_NRT.002

2.2. Spatial analysis

In this research, spatial-autocorrelation is applied for the analysis of the wildland fire patterns. The spatial autocorrelation of wildland fire refers to the degree to which the occurrence or intensity of fires in one area is correlated with that of neighbouring areas. This analysis can provide valuable insights into the underlying processes driving wildland fire dynamics. In brief, spatial auto-correlation is related to the degree to what extent objects or activities in space approximate to others in their vicinity [17]. In spatial statistics, there are many possible ways of measuring spatial auto-correlation by various methods. In this study, Moran's I, arguably the most used method in practice for the analysis of global spatial autocorrelation, is applied for the indication of clustering in the given dataset [18]. Moran's I values range from -1 to 1, where: a Moran's I value close to 1 indicates positive spatial autocorrelation, meaning that similar values tend to cluster together in space, a Moran's I value close to -1 indicates negative spatial autocorrelation, meaning that dissimilar values tend to be located near each other in space, and a Moran's I value close to 0 suggests no spatial autocorrelation, indicating a random spatial pattern where values are not related to their spatial proximity.

Local Indicators of Spatial Association (LISA), Local Moran I, is used to identify spatial clusters [19]. Local Moran's I is important for finding local clusters of high values (high-high clusters) or low values (low-low clusters), as well as geographical outliers (high-low or low-high clusters). This information is useful for understanding geographical patterns and processes that may not be apparent from global assessments of spatial autocorrelation alone.

For the purpose of this study spatial database is created in free and open access and open source Geographic Information System software QGIS3.4[3]. The fire data, presented as point vectors are overlapped with NUT2 administrative vector polygons representing municipalities. Using function count points by polygon all the registered fire pixels belonging to a certain territory are collected and the total number of fires is assigned as an attribute to the relevant municipality. Moran's I and Local Moran's I are computed in GeoDa[4], a free software package for spatial data analysis, geo-visualization, spatial autocorrelation and spatial modelling.

3. Results and Discussion

3.1. Moran's I analysis results

For conducting Moran's I statistical test, first order queen contiguity is applied for defining the spatial weights (i.e. relationships). In order to achieve robust estimates of statistical significance 9999 permutations are conducted. Permutations are used in spatial analysis to construct a test statistic distribution based on the null hypothesis of no spatial autocorrelation. Permutations generate a reference distribution by randomly shuffling the variable's values across geographic locations, and assist in determining if the observed spatial pattern in the data is statistically significant or merely the result of random chance.

The analysis is conducted for the cumulative period from 2013-2023, but also it looks at changes over the five-year period, in order to understand spatial-temporal changes, i.e., considering 2013, 2018 and 2023. Results of the global autocorrelation show a statistically

---

[3] https://www.qgis.org/en/site/
[4] https://spatial.uchicago.edu/geoda

significant spatial autocorrelation for all periods observed, i.e., the null hypothesis of no spatial autocorrelation, is rejected (Table 1). Therefore, the LISA method is used to identify spatial clusters.

Table 1 Results of the global autocorrelation (Moran's I)

Year	Moran's I	p-value	Z-value
2013	0.290	0.0001	6.679
2018	0.507	0.0001	11.628
2023	0.162	0.0045	4.0993
2013-2023	0.281	0.0001	6.894

3.2. Anselin Local Moran's I Cluster (LISA) and Outlier analysis results

Geographically, wildland fires are unequally distributed in Serbia. Most of them, over 60%, are detected in the province of Vojvodina, about 10 % in the province of Kosovo and Metohija, and the rest in Central Serbia. Cluster and Outlier analysis (Anselin Local Morans) reveals clusters of High (HH), and Low (LL) values, as well as outliers where municipalities with high values are surrounded by municipalities with low values (HL) and vice versa (LH).

The concentration of HH clusters is predominantly in the northern and central regions of Serbia. This suggests a regional pattern where certain municipalities are more prone to wildland fire incidents. Some municipalities, shift over time, such as Negotin and Smederevo, since they show up in individual years (2013 and 2018, respectively) but do not appear consistently in the long-term analysis.

As it can be seen from the Fig. 1, the spatial distribution of the identified clusters, as well as the number of municipalities that form them, differs over the observed periods. For instance comparing 2013 and 2018, with 2023, we can observe significantly more prominent HH clusters in 2013 and 2018, with 22, and 27 municipalities clustered, than in 2023, with only 12 municipalities forming two spatial clusters. This can point to similar spatial-temporal underlying causes like climate conditions in the clustered municipalities (for instance drought events).

However, considering the entire period (2013-2023) trend points to HH clusters concentrated largely in the eastern part of Vojvodina province, containing 19 municipalities forming one large cluster. Požarevac, Bogatić, Kikinda, Žitište, Sečanj, Šid, Irig, Ruma, and Stara Pazova appear consistently across all observed periods, indicating persistent high wildland fire incidents in these municipalities. On the other hand, Titel, Alibunar, Kovačica, Kovin, Opovo, Pančevo, Plandište, Nova Crnja, Zrenjanin, and Inđija are also consistently present in the long-term analysis (2013-2023).

LH clusters are municipalities with low numbers of fire incidents surrounded by neighbouring municipalities with high numbers of fire incidents. This spatial relationship is indicative of areas that may benefit from regional fire management practices despite having fewer incidents themselves. For instance, Grocka, Beočin, and Velika Plana appear consistently across multiple periods, suggesting a persistent pattern where these municipalities experience fewer fires relative to their neighbours. Other municipalities, such as Majdanpek, Temerin, Vladimirci, Despotovac, Boljevac, Zaječar, Palilula, Mladenovac, Kovin, and Pančevo, show up in specific years but not consistently across all periods. LH clusters highlight municipalities that, despite having low incident rates, are situated in high-risk regions. For instance, Bela Crkva with 330 wildland fire incidents in the 2013-2023 period, borders Kovin with 1274 wildland fire incidents. These areas are critical for understanding the broader regional dynamics of fire incidents. The presence of high incident rates in neighbouring municipalities suggests potential spillover effects or shared risk factors that could influence the wildland fire risk in LH municipalities.

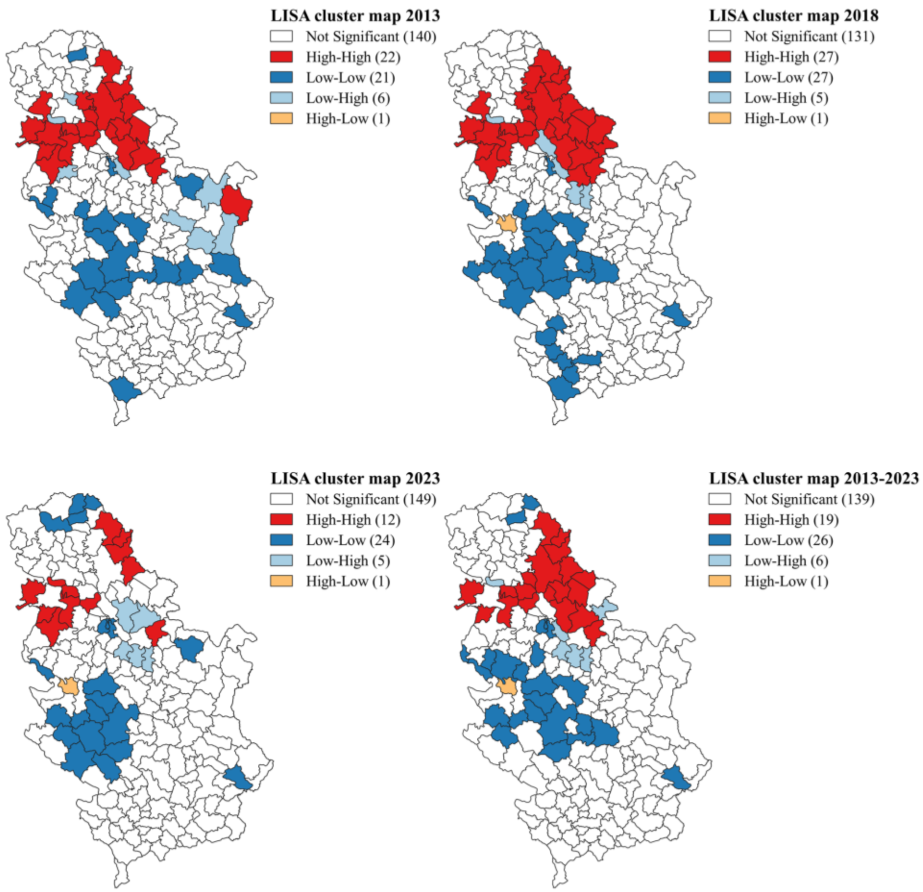

Fig. 1 Cluster and Outlier analysis (Anselin Local Moran's I)

HL clusters represent municipalities with high numbers of wildland fire incidents surrounded by neighbouring municipalities with low numbers of fire incidents. This pattern suggests that the municipality is an outlier in its region, experiencing significantly more wildland fire incidents compared to its neighbours.

Kosjerić is the only municipality identified as a High-Low cluster in both 2018 and 2023, and consistently across the entire period from 2013 to 2023. This suggests a persistent anomaly where Kosjerić consistently experiences a high number of fire incidents despite its neighbouring areas having low incidents. The persistent HL clustering of Kosjerić indicates that it has unique risk factors or conditions leading to higher wildland fire incidents compared to its surroundings. This isolation requires a focused investigation into local conditions. The absence of other HL clusters underscores the distinctiveness of Kosjerić's situation. Understanding why Kosjerić deviates from regional norms can provide insights into specific local vulnerabilities.

3.3. High Incident vs. High-High Clusters

High wildland fire incident counts do not automatically translate to HH clusters. Factors like geographical spread, neighbouring municipality fire incidents, and local conditions play significant roles in forming clusters. Some municipalities, such as Smederevo and S. Mitrovica (Table 2), consistently report high numbers of fire incidents but do not always form HH clusters. This suggests that while these areas experience many fires, they may not have the same spatial clustering as other areas. The presence of HH clusters indicates areas where wildland fire incidents are not only frequent but also geographically concentrated. This spatial concentration can be critical for identifying regions that may benefit from targeted fire prevention and management strategies. HH clusters show spatial dependence, meaning that fire incidents in these areas are likely influenced by incidents in neighbouring municipalities. This dependence is crucial for understanding and addressing the underlying causes of fire incidents.

Table 2 Top ten municipalities according to the number of wildland fire incidents

2013	2018	2023	2013-2023
Bor (338)	Smederevo (918)	Smederevo (460)	Smederevo (5780)
S. Mitrovica (321)	Zrenjanin (740)	S. Mitrovica (274)	S. Mitrovica (2553)
Smederevo (297)	S. Mitrovica (618)	Žitište (267)	Zrenjanin (2471)
Zrenjanin (279)	Pančevo (492)	Ruma (174)	Žitište (2318)
Ruma (246)	Kovačica (465)	Zrenjanin (143)	Vršac (1922)
Žitište (206)	Kovin (439)	Pećinci (134)	Ruma (1880)
Paraćin (184)	Žitište (435)	Cršac (98)	Pančevo (1574)
Pećinci (155)	Vršac (426)	Glogovac (98)	Paraćin (1531)
Kovin (152)	Ruma (425)	Bor (79)	Sečanj (1414)

5. CONCLUDING REMARKS

The spatial patterns identified through Anselin Local Moran's I analysis highlight the importance of considering spatial relationships and neighbouring influences in wildland fire incident management. By integrating these insights into fire management policies, authorities can allocate resources more effectively, tailor interventions to local conditions, and enhance overall fire prevention and response strategies.

The spatial autocorrelation analysis of fire incidents in Serbia from 2013 to 2023 reveals significant spatial patterns that provide valuable insights for policy and management interventions. By examining HH, LH, and HL clusters, several key conclusions and recommendations emerge for enhancing wildland fire management and prevention strategies: 1) Municipalities consistently forming HH clusters, such as Požarevac, Bogatić, Kikinda, Žitište, Sečanj, Šid, Irig, Ruma, and Stara Pazova, should be prioritized for fire management resources due to their spatial concentration of incidents. Investigating the underlying causes for persistent high fire incidents in these municipalities, including factors such as vegetation type, land use, climate conditions, and human activities, will aid in creating effective prevention measures; 2) Municipalities forming LH clusters, such as Grocka, Beočin, and Velika Plana, should be integrated into broader regional fire management strategies. Despite having fewer incidents themselves, they are situated in high-risk regions; 3) consistent identification of Kosjerić as a High-Low cluster indicates a persistent anomaly where this municipality experiences significantly higher fire incidents compared to its neighbours.

While the spatial autocorrelation analysis provides valuable insights into the spatial distribution of fire incidents in Serbia, several limitations should be acknowledged: 1) the analysis conducted at the municipal level may mask finer-scale variations in fire incident patterns within municipalities, leading to potential aggregation bias. Municipal boundaries may not accurately reflect the spatial extent of fire risk factors, such as wildland-urban interfaces or ecological boundaries, which could influence the observed spatial patterns; 2) While spatial autocorrelation identifies spatial associations, it does not establish causal relationships between fire incidents and underlying risk factors, requiring additional causal inference methods for deeper understanding; 3) While spatial autocorrelation analysis provides valuable descriptive insights, translating these findings into actionable policy recommendations requires careful interpretation and consideration of practical feasibility.

Therefore, several areas warrant further investigation to enhance understanding of this initial study: 1) Conduct in-depth research to identify the specific causal factors contributing to the spatial patterns observed in HH, LH, and HL clusters; 2) Investigate temporal trends in wildland fire incident patterns to identify any emerging hotspots or shifts in spatial dynamics over time; 3) Develop predictive models for identifying potential future wildland fire hotspots based on historical incident data and environmental variables.

Acknowledgement: *This work was supported by the Serbian Ministry of Science, Technological Development and Innovation through the Mathematical Institute of the Serbian Academy of Sciences and Arts.*

References

1. I. Fuentes-Santos, M. F. Marey-Pérez, and W. González-Manteiga, “Forest fire spatial pattern analysis in Galicia (NW Spain),” J. Environ. Manage., vol. 128, pp. 30–42, 2013, doi: https://doi.org/10.1016/j.jenvman.2013.04.020.
2. N. Fernandez-Anez et al., “Current Wildland Fire Patterns and Challenges in Europe: A Synthesis of National Perspectives,” Air, Soil Water Res., vol. 14, 2021, doi: 10.1177/11786221211028185.
3. J. luc Dupuy et al., “Climate change impact on future wildfire danger and activity in southern Europe: a review,” Ann. For. Sci., vol. 77, no. 2, 2020, doi: 10.1007/s13595-020-00933-5.
4. N. Khabarov et al., “Forest fires and adaptation options in Europe,” Reg. Environ. Chang., vol. 16, no. 1, pp. 21–30, 2016, doi: 10.1007/s10113-014-0621-0.
5. L. Magnusson, C. Prudhomme, F. Di Giuseppe, C. Di Napoli, and F. Pappenberger, “Chapter 2 - Operational multiscale predictions of hazardous events,” in Extreme Weather Forecasting, M. Astitha and E. B. T.-E. W. F. Nikolopoulos, Eds. Elsevier, 2023, pp. 87–129.
6. E. Chuvieco and J. Salas, “Mapping the spatial distribution of forest fire danger using GIS,” Int. J. Geogr. Inf. Syst., vol. 10, no. 3, pp. 333–345, 1996, doi: 10.1080/02693799608902082.
7. H. Abedi Gheshlaghi, “Using GIS to Develop a Model for Forest Fire Risk Mapping,” J. Indian Soc. Remote Sens., vol. 47, no. 7, pp. 1173–1185, 2019, doi: 10.1007/s12524-019-00981-z.
8. “https://www.earthdata.nasa.gov/learn/find-data/near-real-time/firms.” .
9. N. Levin and A. Heimowitz, “Mapping spatial and temporal patterns of Mediterranean wildfires from MODIS,” Remote Sens. Environ., vol. 126, pp. 12–26, 2012, doi: 10.1016/j.rse.2012.08.003.

10. Salma et al., "Prediction capability of the MCDA-AHP model in wildfire risk zonation of a protected area in the Southern Western Ghats," Environ. Sustain., vol. 6, no. 1, pp. 59–72, 2023, doi: 10.1007/s42398-022-00259-0.
11. S. Nikhil et al., "Application of GIS and AHP Method in Forest Fire Risk Zone Mapping: a Study of the Parambikulam Tiger Reserve, Kerala, India," J. Geovisualization Spat. Anal., vol. 5, no. 1, p. 14, 2021, doi: 10.1007/s41651-021-00082-x.
12. F. Sivrikaya and Ö. Küçük, "Modeling forest fire risk based on GIS-based analytical hierarchy process and statistical analysis in Mediterranean region," Ecol. Inform., vol. 68, no. November 2021, 2022, doi: 10.1016/j.ecoinf.2021.101537.
13. M. L. Chas-Amil, J. Touza, and E. García-Martínez, "Forest fires in the wildland-urban interface: A spatial analysis of forest fragmentation and human impacts," Appl. Geogr., vol. 43, pp. 127–137, 2013, doi: 10.1016/j.apgeog.2013.06.010.
14. M. H. Nami, A. Jaafari, M. Fallah, and S. Nabiuni, "Spatial prediction of wildfire probability in the Hyrcanian ecoregion using evidential belief function model and GIS," Int. J. Environ. Sci. Technol., vol. 15, no. 2, pp. 373–384, 2018, doi: 10.1007/s13762-017-1371-6.
15. Z. X. Zhang, H. Y. Zhang, and D. W. Zhou, "Using GIS spatial analysis and logistic regression to predict the probabilities of human-caused grassland fires," J. Arid Environ., vol. 74, no. 3, pp. 386–393, 2010, doi: 10.1016/j.jaridenv.2009.09.024.
16. P. Vranić, S. Glišović, and L. Velimirović, "Decision Support for Integrated Management of Local-Level Adaptation to Climate Changes: The Case of Serbia," Int. J. Disaster Risk Sci., vol. 12, no. 4, pp. 479–494, 2021, doi: 10.1007/s13753-021-00357-3.
17. M. F. Goodchild, Spatial Autocorrelation. University of California, 1986. ISBN 0860942236.
18. P. A. P. Moran, "The Interpretation of Statistical Maps," Journal of the Royal Statistical Society: Series B (Methodological), vol. 10, no. 2, pp. 243–251, July 1948, doi: https://doi.org/10.1111/j.2517-6161.1948.tb00012.x.
19. L. Anselin, "Local indicators of spatial association—LISA," Geographical Analysis, vol. 27, no. 2, pp. 93-115, 1995, doi: https://doi.org/10.1111/j.1538-4632.1995.tb00338.x.

ANALIZA PROSTORNE DISTRIBUCIJE INCIDENTA POŽARA U SRBIJI NA OSNOVU PODATAKA VIIRS 375 M ZA PERIOD 2013-2023.

Ovo istraživanje analizira prostornu distribuciju i obrasce klastera požara u divljini u Srbiji od januara 2013. do decembra 2023. koristeći podatke dobijene iz NASA-inog Sistema informacija o požarima za upravljanje resursima (FIRMS). Ukupno 69179 požara je mapirano pomoću Visible Infrared Imaging Radiometer Suite (VIIRS) 375 m. Analiza prostorne autokorelacije, posebno Moran I i Lokal Morans I, je primenjena da bi se procenio stepen grupisanja mapiranih požara. Rezultati ukazuju na značajne prostorne obrasce, ističući kritične oblasti za upravljanje i prevenciju požara. Opštine Požarevac, Bogatić, Kikinda, Žitište, Sečanj, Šid, Irig, Ruma i Stara Pazova, su identifikovane kao "High-High" klasteri. "Low-High" klaster, uključujuje Grocku, Beočin i Veliku Planu. Pored toga, "High-Low" klaster u Kosjeriću ukazuje na anomaliju koja zahteva fokusiranu intervenciju. Ovi uvidi pružaju korisne informacije za fokusirane strategije upravljanja požarima i ističu važnost prostorne analize u razumevanju dinamike požara.

Ključne reči: *divlji požari, prostorna analiza, klasterovanje, Moran's I, Local Moran's I, Srbija*

FACTA UNIVERSITATIS
Series: **Working and Living Environmental Protection** Vol. 21, Nº 2, 2024, pp. 97 - 107
https://doi.org/10.22190/FUWLEP240712009D

Original Scientific Paper

ASSESSMENT OF ECOLOGICAL RISK IN THE PAINT AND COATINGS INDUSTRY FROM THE PERSPECTIVE OF THE AQUATIC ECOSYSTEM

UDC 502/504[061.5:667

Amelija Đorđević[1], Danijela Stojadinović[2], Ana Stojković[1], Ivan Krstić[1]

[1]University of Niš, Faculty of Occupational Safety, Niš, Serbia
[2]Academy of Vocational Studies South Serbia,
Department for Technological and Artistic Studies in Leskovac, Serbia

ORCID iDs:	Amelija Đorđević	https://orcid.org/0000-0002-3260-2626
	Danijela Stojadinović	https://orcid.org/0000-0002-6335-8101
	Ana Stojković	https://orcid.org/0000-0002-2043-7424
	Ivan Krstić	https://orcid.org/0000-0001-7181-0885

Abstract. *In assessing ecological risk in the paint and coatings industry, stressors are examined from the perspective of exposed hazardous substances, whether as input substances or substances leaving the technological process and entering the environment. The extent of their negative impact on humans, living organisms, non-living nature, and material goods depends on their characteristics and the frequency and degree of their effects. When assessing risks, the frequency and degree of their effects are considered in terms of regular operational regimes and accident scenarios. The spatial distribution of hazardous substances reaching watercourses is also presented based on calculations of maximum emission quantities and volumes of substances, as well as the determination of the area of contaminated watercourses. Risk is assessed concerning the probability of the most likely unwanted events in the paint and coatings industry and their consequences for human life, health, and the environment.*

Key words: *ecological risk, paint and coatings industry, aquatic ecosystem*

1. INTRODUCTION

Ecological hazard is the probability of compromising human health and environmental conditions due to uncontrolled emissions of pollutants. Environmental risk includes risks that endanger the health and lives of people, as well as risks that threaten the condition of the environment. It can result from various technological processes applied in the chemical industry, among other factors. The assessment of ecological risk arising in the chemical

Received July 12, 2024 / Accepted October 16, 2024
Corresponding author: Ana Stojković
Faculty of Occupational Safety, Univesity of Niš, Čarnojevića 10a, 18000 Niš, Serbia
E-mail: ana.stojkovic@znrfak.ni.ac.rs

industry is linked to the consequences resulting from the actions of hazardous substances on ecosystems, which are inherently complex.

The technological processes used in the paint and coatings industry, as part of the chemical industry, are heterogeneous. The raw materials and intermediates used vary in terms of the hazards and damages they can cause during different accident scenarios. The production of paints and coatings represents the culmination of a highly complex chemical industry chain. Within this chain, pigments of organic or inorganic origin are synthesized, followed by polymers used in paint production, and finally, solvents that serve as the base for paints and coatings.

During the operation of this industry, as well as in accident scenarios, various pollutants are released into water, air, and soil. A particular risk in the paint and coatings industry is the release, spillage, or leakage of hazardous substances that often reach surface watercourses uncontrollably. The extent of degradation of watercourses depends on the transformation of hazardous substances into harmful ones. The conversion of hazardous substances into harmful ones depends on the physicochemical and toxicological characteristics of the substances, as well as their quantities and the specific characteristics of the watercourses themselves.

Understanding the chemical composition and physicochemical properties of input substances and substances leaving the technological process and entering the environment is fundamental for assessing ecological risk during regular operations and in accident scenarios.

2. THE PRESENCE OF HAZARDOUS SUBSTANCES IN WATERCOURSES

Hazardous substances used in the paint and coatings industry can enter watercourses as part of wastewater or in the event of accidental (incidental) incidents. Wastewater is generated in the processes of washing and cleaning production areas and equipment, and its quality depends on the properties of the substances used in the production process. It can also originate from the process of caustic cleaning of tanks and secondary pipelines. Wastewater in the paint and coatings industry is typically alkaline in nature, with a small percentage of oils and fats, and characterized by low BOD (Biological Oxygen Demand) values. Wastewater can have high COD (Chemical Oxygen Demand) values due to the presence of organic substances used, such as solvents, preservatives, styrene, acetone, benzene, phenol, etc. Additionally, liquid waste may contain residues of heavy metals that come from the pigments used. All paints contain pigments in their composition, which are natural or synthetic compounds. Pigments are powdery substances that can be most simply classified as organic and inorganic; they are soluble in water, alcohol, or oil used in the technological process. Table 1 presents the classification of inorganic pigments. Synthetic organic pigments are hydrocarbon compounds and can have varying degrees of toxicity [1].

Table 1 Classification of inorganic pigments based on chemical composition

Compounds	Chemical formula
Oxide pigments	TiO_2, ZnO, α-Fe_2O_3, α-FeOOH, γ-Fe_2O_3, Fe_3O_4, Cr_2O_3, CrOOH, PbO, Pb_3O_4, Mn_3O_4, -MnOOH, Sb_2O_3
Complex oxide	$CoAl_2O_4$, $CuCr_2O_4$, Co_2TiO_4, $(Ti,Ni,Sb)O_2$, $(Ti,Cr,Sb)O_2$
Carbonate hydroxide	$2PbCO_3 \cdot Pb(OH)_2$, $2CuCO_3 \cdot Cu(OH)_2$, $CuCO_3 \cdot Cu(OH)_2$
Sulphide, selenium	ZnS, CdS, Cd(S,Se), CdSe, γ-Ce_2S_3, HgS, As_2S_3
Chromate, molybdate	$PbCrO_4$, $Pb(Cr,S)O_4$, $Pb(Cr,S,Mo)O_4$, $ZnCrO_4$, $BaCrO_4$, $SrCrO_4$
Bismuth	$BiVO_4$, $4BiVO_4 \cdot 3Bi_2MoO_6$
Tin	Pb_2SnO_4, $PbSn_2SiO_7$, Co_2SnO_4, $CoSnO_3$
Phosphate	$Co_3(PO_4)_2$
Antimony	$Pb(SbO_3)_2$
Arsenic	$Cu(AsO_3)_2$
Ultramarine	$Na_6Al_6Si_6O_{24}(NaS_n)$
Hexacyanoferrate	$K[Fe^{III}Fe^{II}(CN)_6] \cdot xH_2O$ ($x = 14$–16)
Tantalum oxide	$CaTaO_2N$, $LaTaON_2$
Elements	C, Al, Cu, Cu/Zn, Au

Determining the maximum amount of pigments in the composition of wastewater, as well as solvents or other hazardous substances, can be considered one of the relevant factors in risk assessment. Hazardous substances such as chromium, copper, lead, zinc, titanium, and others cannot be found in their original form in the influent because, during the production process, they mix with various other substances and solvents.

The largest amount of wastewater from the paint and coatings industry is generated from equipment cleaning, accounting for about 80% of the influent. According to statistical data, approximately 70% of wastewater from the paint and coatings industry is discharged untreated into natural river basins and contains hazardous substances that vary in their solubility, volatility, and toxicity [2,11].

In the event of an accidental incident, a spill or leak of hazardous substances can occur, leading to their release into watercourses in their original form. The degradation of the watercourses will depend on the toxicity level, quantity, volume, and area of the contaminated watercourses, as well as the exposure time.

3. Risk Assessment

Assuming that an accidental event or incident in the chemical industry occurs as a result of a leak of hazardous substances, the risk can be modeled as the product of the number of participants in the scenario and the frequency of the incident.

risk = frequency of the incident x number of participants in the scenario

The frequency of accidents is analyzed using data from the following dataset:

1. Reliability data was prepared by determining accident and equipment failure data in the factory.
2. Equipment failure frequency data provided by equipment manufacturers.
3. Reliability data provided by the European reliability database for industry.
4. Reliability data for non-electronic components.

Representative data on the frequency of most likely accidents related to the paint and coatings industry are presented in Table 2 [3].

Table 2 Annual frequency of accidents

Initial event	Known probabilities of events (on an annual basis)
Court cancellation under pressure	10^{-6}
Pipeline failure due to malfunction (at 100 m)	10^{-5}
Pipeline leak (at 100 m)	10^{-3}
Atmospheric tank failure	10^{-3}
Flange/valve leak	10^{-3}
Pump/compressor leak	10^{-3}
Premature opening of the spring valve	10^{-2}
Malfunction during water cooling	10^{-1}
Discharge/filling hose failure	10^{-2}
External fire	10^{-2}

In the Republic of Serbia, there is no available systematic database regarding accidents and malfunctions of equipment and facilities in the paint and varnish industry, so the risk assessment of each plant can be performed using the REHRA method, according to the scheme given in Figure 1.

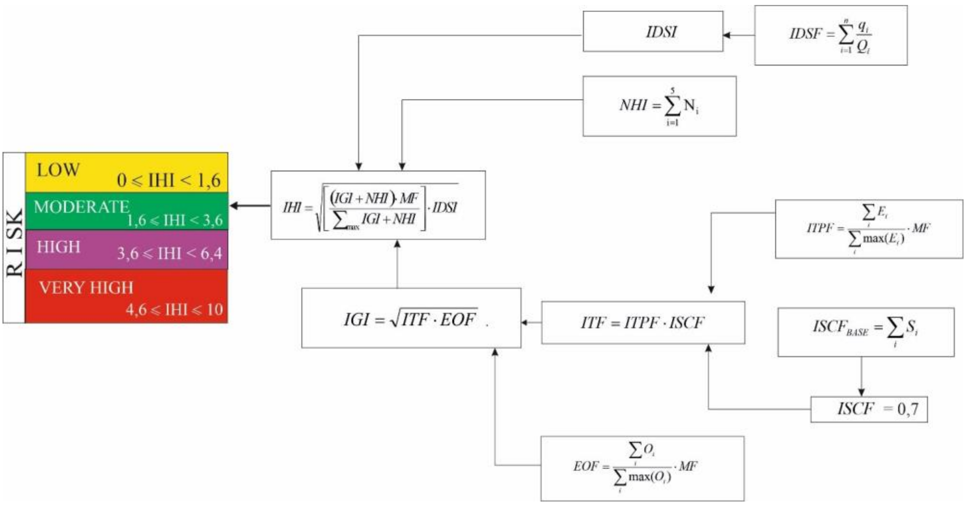

Fig.1 Summary of risk assessment within facilities applied in the industry [2,5]

Calculation of the number of participants in the scenario is based on establishing the boundaries of hazardous substance leakage so that the leakage zone defines the radius from the source of leakage to the furthest point of dispersion. The level of potential adverse consequences resulting from the entry of hazardous substances into watercourses can be determined by identifying the maximum quantities of substances entering the watercourses and determining the volume they occupy in the watercourses.

The maximum amount of hazardous substances that can be released into a surface watercourse is determined by Equation 1. [4,5]

$$Q_{ws} = Q \times f_1 \times f_2 \tag{1}$$

Q_{WS} is the maximum mass of a substance that can reach water or soil after its release.
Q is the maximum quantity of a given substance that can be discharged from the equipment (in tons).
f_1 is the reduction coefficient based on the physical properties of the released substance.
f_2 is the reduction coefficient associated with technical protective measures aimed at retaining discharged hazardous substances from the facility.

The reduction coefficients are determined according to Tables 3 and 4, and their values range from 0 to 1.

Table 3 Criteria for selecting the value of reduction coefficient f_1

f_1	Description
1	If the boiling point of the substance at atmospheric pressure is higher than 55°C
1 - 0.75	If the boiling point of the substance at atmospheric pressure is between 21°C and 55°C
0.75 - 0.5	If the boiling point of the substance at atmospheric pressure is between 0°C and 21°C
0.5 - 0.2	If the boiling point of the substance at atmospheric pressure is between -35°C and 0°C
0.2 - 0	f the boiling point of the substance at atmospheric pressure is below -35°C

Table 4 Criteria for selecting the value of coefficient f_2

f_2	Description
1	If the spillage goes directly into the final receptor (soil or watercourse) without any protective barrier
1 - 0.8	If the spillage does not go directly into the final receptor (soil or watercourse), but it's not possible to divert the contents to a separate treatment system or retention basin
0.8 - 0.4	If part of the spilled contents can be directed to a collection system or can be retained in a retention basin
0.4 - 0.1	If there is a spillage in the retention basin or if a larger portion of the spilled contents can be directed, treated, or somehow recovered

To conduct a relevant risk assessment for the discharge of hazardous substances into surface waters, in addition to determining the volume of contaminated water, the possibility of spreading (spillage) of hazardous substances is also considered. The extent of contamination of watercourses primarily depends on the physical properties of the substances and the presence of specific barriers to the spread of discharged hazardous substances.

To assess the quantity of endangered water, hazardous liquid pollutants are categorized into water-soluble and water-insoluble substances. Water-soluble hazardous pollutants tend to spread homogeneously in watercourses, whereas substances are considered water-insoluble when their solubility is below 10%.

Determining the surface area of watercourses contaminated by the release of water-insoluble liquids is carried out using equation 2 [5,8].

$$W_s = \frac{Q_{ws}}{\rho_s \times d_s} \tag{2}$$

Ws is the surface area of water contaminated by the discharge of water-insoluble liquids (m^3).
d_s is the average thickness of the substance layer on the surface of the watercourse (m).
ρ_s is the density of the discharged substance (kg/m^3).

Calculating the volume of contaminated water affected by toxic substances discharged from industry is done using equation 3 [4,5].

$$V = \frac{Q_{rws}}{LC_{50} \times P \times BCF} \tag{3}$$

V is the volume of contaminated water (m^3).
Q_{rws} is the maximum amount of substance reaching the water (g).
LC_{50} is the lethal concentration (mg/dm^3).
P is the persistence factor (dimensionless).
BCF is the bioconcentration factor (dimensionless).

To determine the ecological risk arising from the discharge of hazardous substances into watercourses, Equations 1 and 2 (REHRA) can be applied.

In case of an accidental event, organic solvents of varying toxicity levels can be discharged into watercourses. Table 5 provides the maximum quantity of organic solvents that can be released into watercourses during accidents, determined using Equation 1. To calculate the maximum quantity that can be found in the watercourse, data on the maximum permitted quantities of substances used in production according to SEVESO plant regulations are used. A substance that reaches watercourses and dissolves in water immediately can endanger the watercourse depending on its toxicity. The volume of surface water that is endangered in such cases can be determined using Equation 3 and is provided in Table 5.

Based on the calculations provided in Table 5, it can be concluded that the maximum mass of substance released into watercourses can be reduced by a factor of ten, depending on whether there are specific systems for collecting the discharged substance or if it is directly discharged into watercourses. If there is a spillage in the retention basin or if a larger portion of the spilled content can be directed, treated, or somehow recovered, the mass of discharged substance into watercourses during an accidental event can be reduced by a factor of ten.

To predict or assess the risk resulting from the discharge of hazardous substances into surface waters, it is crucial to determine the volume of endangered (contaminated) water for which damage is assessed according to Tables 6 and 7. After determining the consequences or damage of the unwanted event, as well as the probability of its occurrence according to Table 8, a risk matrix is formed as shown in Figure 2. [6]

Table 5 Quantity of discharged substance into the surface watercourse and volume of endangered water [2]

Substance	If the spillage goes directly into the final receptor (soil or watercourse) without any protective barrier		If the spillage does not go directly into the final receptor (soil or watercourse), but it's not possible to divert the contents to a separate treatment system or retention basin		If the spilled content can be directed to a collection system or retained in a retention basin		If there is a spillage in the retention basin or if a larger portion of the spilled content can be directed, treated, or somehow recovered	
	Q_{WS} (t)	V (m^3)	Q_{WS} (t)	V (m^3)	Q_{WS} (t)	V (m^3)	Q_{WS} (t)	V (m^3)
Aromatic hydrocarbons								
Benzene C_6H_6	50	3.88	40	310	20	1.55	5	0.39
Toluene C_6H_6	50	7.05	40	5.64	20	2.82	5	0.71
Xylene C_8H_{10}	50	6.58	40	5.27	20	2.63	5	0.66
Naphthalene $C_{10}H_8$	50	11.5	40	9	20	4.5	5	0.75
Alcohols								
Methanol CH_4O	50	0	40	0	20	0	5	0
Ethanol C_2H_6O	50	0.01	40	0.01	20	0	5	0
Propanol C_3H_8O	50	0.01	40	0.01	20	0.01	5	0
n-Butanol $C_4H_{10}O$	50	0.05	40	0.04	20	0.02	5	0
Amyl alcohol $C_5H_{12}O$	50	0.10	40	0.08	20	0.04	5	0.01
Cyclo-hexanol $C_6H_{12}O$	50	0.09	40	0.08	20	0.04	5	0.01
Ethylene glycol $C_2H_6O_2$	50	0	40	0	20	0	5	0
Benzyl alcohol C_7H_6O	50	0.14	40	0.12	20	0.06	5	0.01
Etars and acetals								
Ethyl ether $C_4H_{10}O$	42.5	0.02	34	0.01	17	0.01	4.25	0
n-Propyl ether $C_6H_{14}O$	50	263.16	40	210.53	20	105.26	5	26.32
Dioxane $C_4H_8O_2$	50	0.49	40	0.39	20	0.19	5	0.05
Aldehydes and ketone								
Aceta-ldehyde C_2H_4O	36.5	1.07	29.2	0.86	15	0.44	3.65	0.11
Acrolein C_3H_4O	45	2368.42	36	1894.74	18	947.37	4.5	236.84
Furfural $C_5H_4O_2$	36	1,5	28.8	1.18	14.4	0.60	3.6	0.5

Acetone C_3H_6O	50	0.01	40	0.01	20	0	5	0
Acetic acid $C_2H_4O_2$	50	0.57	40	0.45	20	0.23	5	0.06
Formic acid HCOOH	50	0.38	40	0.31	20	0.15	5	0.04
Esthers								
Methyl formate $C_2H_4O_2$	41	0.46	32.8	0.36	16.4	0.18	4.1	0.05
Ethyl formate $C_3H_6O_2$	47.5	0.28	38	0.22	19	0.11	4.8	0.03
Butyl formate $C_5H_{10}O_2$	50	1.84	40	1.47	20	0.73	5	0.18
Methyl acetate $C_3H_6O_2$	50	0.19	40	0.15	20	0.08	5	0.02
Ethyl acetate $C_4H_8O_2$	50	0.29	40	0.23	20	0.12	5	0.03
Chlorinated hydrocarbons								
Chloroform$CHCl_3$	50	0.44	40	0.35	20	0.17	5	0.04
Carbon tetrachloride CCl_4	50	5.49	40	4.39	20	2.19	5	0.55
Dichloro-ethane $C_2H_4Cl_2$	50	0,.44	40	0.36	20	0.18	5	0.04
Trichloro-Ethylene C_2HCl_3	50	3.25	40	2.6	20	1.3	5	0.33
Tetrachloro-ethylene C_2Cl_4	50	7.25	40	5.8	20	2.98	5	2.72
Chloro-benzene C_6H_5Cl	50	0.69	40	0.55	20	0.28	5	0.07
Organic nitrogen compounds								
Aniline C_6H_7N	50	4.72	40	3.77	20	1.89	5	0.47
m-Toluidine C_7H_9N	50	1.38	40	1.10	20	0.55	5	0.14
Pyridine C_5H_5N	50	0.53	40	0.43	20	0.21	5	0.05
Acetonitrile C_2H_3N	50	0.03	40	0.02	20	0.01	5	0
Nitro-benzene $C_6H_5O_2N$	50	0.54	40	0.43	20	0.22	5	0.05
Organic sulfur compounds								
Carbon disulfide CS_2	47	15.67	37.6	12.53	18.8	6.27	4.7	1.37
Compounds with multiple functional groups								
Methylene glycol $C_3N_8O_2$	50	0.43	40	0.34	20	0.17	5	0.04
Ethylene glycol $C_4N_{10}O_2$	50	0	40	0	20	0	5	0
Diethylene glycol $C_4N_{10}O_3$	50	0	40	0	20	0	5	0
o-Chloro-aniline C_6N_6ClN	50	11.70	40	9.36	20	4.68	5	1.17

Table 6 Categorization of consequences on human life and health

Consequences on human life and health			
Category	Extent of consequences	Criterion *	Selected
1	Minimal	<50	
2	Minor	50-200	
3	Moderate	201-500	
4	Severe	501-1500	
5	Catastrophic	>1500	

*Total number of people affected by a hazard (deceased, injured, ill, evacuated, displaced - homeless, accommodated, and sheltered)

Table 7 Categorization of consequences for economy/ecology

Consequences for economy/ecology			
Category	Extent of consequences	Criterion **	Selected
1	Minimal	exceeding 1% of the budget	
2	Minor	exceeding 3% of the budget	
3	Moderate	exceeding 5% of the budget	
4	Severe	exceeding 10% of the budget	
5	Catastrophic	exceeding 15% of the budget	

**Total costs include healthcare or medical treatment costs, immediate or long-term emergency measures, building restoration costs, public transport and infrastructure costs, material goods, cultural heritage, ecological restoration costs, costs of business interruption, and insurance premiums paid.

At the national level, economic/ecological consequences are assessed relative to the budget of the Republic of Serbia.

At the level of autonomous provinces and local self-governments, economic/ecological consequences are assessed relative to the budgets of autonomous provinces and local municipalities.

Consequences for companies and other legal entities are expressed as the sum of fixed assets and working capital values, calculated as a percentage according to the categories mentioned above.

Table 8 Categorization of the probability of occurrence of a hazardous event

Probability or frequency				
Category	a) Qualitative	b) Qualitative	c) Qualitative	Selected
1	Negligible	< 1 %	1 event in 100 years or less	
2	Low	1 - 5 %	1 event in 20 to 100 years	
3	Moderate	6 - 50 %	1 event in 2 to 20 years	
4	High	51- 98 %	1 event in 1 to 2 years	
5	Very high	> 98 %	1 event annually	

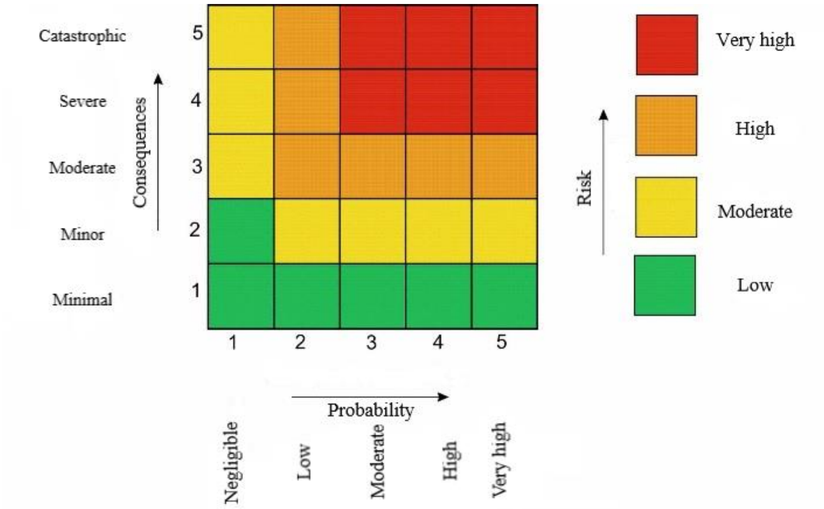

Fig. 2 Risk Assessment Matrix according to the methodology of the Republic of Serbia

Therefore, the risk to the aquatic ecosystem can be determined as the product of the probability of occurrence of the unwanted event (P) and the resulting damage or consequences (W), according to Equation 4 [6, 7].

$$R = P \times W \tag{4}$$

Assessing risk is essential for making decisions regarding the need to implement risk management procedures.

4. CONCLUSION

In the production of paints and coatings, a wide range of substances with varying properties and characteristics are used, many of which fall into the category of hazardous substances. Comparing substances within this group, it is concluded that the most significant ecological risks are associated with the emission of organic solvents and pigments, which can enter watercourses during accidental events. The quantity, volume, and area of contaminated water can be determined using the REHRA methodology. Ecological risk assessment relative to contaminated water involves evaluating the probability of an undesirable event leading to the release of hazardous substances into watercourses and the resulting environmental and health impacts on exposed populations. The probability and consequences, treated as damage, are determined according to the methodology. Calculations show that the maximum mass of substances released into watercourses can be reduced by up to tenfold depending on whether specific collection systems are in place for the discharged substances or if they are directly released into watercourses. If containment basins are used or if a significant portion of the spilled content can be removed, treated, or otherwise recovered, the mass of released organic solvents into watercourses during an accident can also be reduced by up to tenfold.

Acknowledgement: *This paper is a part of the research funded by the Ministry of Education, Science and Technological Development of the Republic of Serbia pursuant to agreement No. 451-03-66/2024-03/ 200148.*

REFERENCES

1. https://www.atsdr.cdc.gov/toxprofiles/tp3.pdf
2. Stojadinović D. (2023). Razvoj metodologije koordinacije procene i upravljanja ekološkim rizikom u industriji boja i lakova. Doktorska disertacija. Fakultet zaštite na radu u Nišu, Univerzitet u Nišu
3. Lee H. E, Kim M. G, Yoon S. J, Huh D. A, Moon K. W. (2021). Changes in Risk in Medium Business Plating and Paint Manufacturing Plants following the Revision of the Korean Chemical Accident Prevention System. *International Journal of Environmental Research and Public Health*, 18, 11982.
4. Quick assessment of risk to the environment and health, Rehra 2. (2003). Ministry for the environment and territory
5. Đorđević A, Stevanović V. (2020). Ekološki rizik. Fakultet zaštite na radu u Nišu. Univerzitet u Nišu. Udžbenik, ISBN 978-86-6093-091-2.
6. Uputstvo o metodologiji izrade i sadržaju procene rizika od katastrofa i plana zaštite i spasavanja *(„Sl. glasnik RS“ br. 80/2019*).
7. Vodič za procenu rizika u svrhe tržišnog nadzora. (2011). WELMEC Evropska saradnja u oblasti zakonske metrologije, vage i merila; WELMEC Secretariat, MIRS Grudnovo nabrezje 17 SI - 1000 Ljubljana
8. Brza procena rizika po životnu sredinu i po zdravlje [*Rapid Environment and Health Risk Assessment*],
9. Vijayaraghavan, G., Kumarm P., Chandrakanthan, K., Selvakumar, S. (2017) Acanthocereus tetragonus an effective natural coagulant for decolorization of synthetic dye wastewater. Journal of Material and Environmental Sciences 8, 3028-3033.
10. Kasperchik, V., Yaskevich, A., Bildyukevich, A. (2012) Wastewater treatment for removal of dyes by coagulation and membrane processes. Petroleum Chemistry 52, 545- 556.
11. Surya Nair K, Basavaraju Manu, Adani Azhoni (2021) Sustainable treatment of paint industry wastewater: Current techniques and challenges. Journal of Environmental Management, Volume 296, Page 113105

PROCENA EKOLOŠKOG RIZIKA U INDUSTRIJI BOJA I LAKOVA SA ASPEKTA VODENOG EKOSISTEMA

Pri proceni ekološkog rizika, u industriji boje i lakova, stresori se posmatraju sa apekta opasnih supstanci koje su u ekspoziciji, a koja se mogu koristiti kao ulazne supstance i supstance koje napuštaju tehnološki proces i dospevaju u životnu sredinu. Koliki će njihov negativni uticaji biti na čoveka, živi svet, neživu prirodu i materijalna dobra zavisi, pored njihovih karakteristika i od učestalosti i stepena njihovog delovanja. Učestalost i stepen njihovog delovanja, pri proceni rizika, u radu se posmatra sa aspekta redovnog režima rada i udesnog događaja. Takođe u radu je prikazana prostorna raspodela opasnih supstanci koje dospevaju do vodotokova na osnovu proračuna maksimalnih količina i zapremina supstanci koje su u emisiji, kao i određivanje površine kontaminiranih vodotokova. Rizik se posmatra u funkciji verovatnoće najverovatnijih neželjenih događaja u industriji boja i lakova i posledica po život i zdravlje ljudi i ekologiju.

Ključne reči: *ekološki rizik, industrija boja i lakova, vodeni ekosistem*

FACTA UNIVERSITATIS
Series: **Working and Living Environmental Protection** Vol. 21, Nº 2, 2024, pp. 109 - 117
https://doi.org/10.22190/FUWLEP240830010S

Original Scientific Paper

FIRE RISK ASSESSMENT IN HAZARDOUS MATERIALS WAREHOUSES

UDC 614.841.47:620.26

Ana Stojković[1], Ivan Krstić[1], Amelija Đorđević[1], Miodrag Stanisavljević[2]

[1]Faculty of Occupational Safety, Niš, Serbia
[2]The Academy of Applied Technical Studies, Department - Applied Engineering Sciences, Požarevac, Serbia

ORCID iDs:	Ana Stojković	https://orcid.org/0000-0002-2043-7424
	Ivan Krstić	https://orcid.org/0000-0001-7181-0885
	Amelija Đorđević	https://orcid.org/0000-0002-3260-2626
	Miodrag Stanisavljević	https://orcid.org/0009-0002-6003-4117

Abstract. *Fire protection in hazardous materials warehouses is based on a complex analysis of calculations and the current state to determine appropriate protection measures. This paper explores the fire hazards associated with storing hazardous materials in a warehouse setting. It provides a detailed assessment of potential risks, focusing on the unique challenges posed by the nature of the materials stored. The study examines various factors that contribute to fire risk, including the flammability of materials, storage conditions, and existing fire prevention measures. The objective is to identify critical vulnerabilities and propose strategies for enhancing safety and reducing the likelihood of fire incidents. The findings aim to inform best practices for managing fire risks in hazardous material storage facilities.*

Key words: *fire risks, assessment, warehouse, hazardous materials.*

1. Introduction

Fire and explosion protection, as a set of preventive and repressive measures and activities, aims to prevent the outbreak and spread of fires, minimize their consequences to the lowest possible level, ensure efficient fire extinguishing, determine the causes and origins of fires and explosions, and assess potential responsibility for failure to take prescribed or required fire and explosion protection measures, as well as detect possible elements of criminal offenses. The ultimate goal is to protect human lives and material

Received August 30, 2024 / Accepted October 11, 2024
Corresponding author: Ana Stojković
Faculty of Occupational Safety, Univesity of Niš, Čarnojevića 10a, 18000 Niš, Serbia
E-mail: ana.stojkovic@znrfak.ni.ac.rs

assets [1]. Fire protection refers to measures taken to reduce the likelihood of damage to material assets or injuries to employees [2,3,4,5]. Preventive measures are crucial for preventing the occurrence of fires and minimizing the consequences they cause [6,7,8]. Due to the concept of prevention, the global fire management paradigm is shifting from damage mitigation to proactive action [9]. Accordingly, fire protection management can be divided into four phases: prevention (mitigation), preparedness, response, and recovery [10]. Prevention methods include continuous education of all stakeholders, fire risk assessment, and improvement of fire response infrastructure [11,12,13]. On the other hand, fire risk assessment involves developing prevention plans considering the likelihood and effects of fire occurrence, prevention costs, and the efficiency and availability of resources [14].

There are various methods and procedures for fire risk assessment [15]. The first group of fire risk assessment procedures originated from the research of Swiss engineer Max Gretenar, conducted between 1961 and 1968. Based on the data obtained, Gretenar formulated a fire risk assessment procedure and defined recommendations for implementing minimum preventive fire protection measures, depending on the fire risk. Gretenar's procedure has been modified in several ways. One version was standardized by the Swiss Association of Insurance Companies in collaboration with the Swiss Association of Engineers and Architects under the name SIA 81, with its latest version, SIA 2007, published in 2007. Another version was developed by the Austrian Fire Brigade Association under the name Technical Recommendation TRVB 100. A modification that differs significantly in its calculation procedure from the previous two was also developed by the European Fire Alarm Manufacturers Association. In Belgium, a fourth modification known as FRAME (Fire Risk Assessment Method for Engineering) was developed in 1988. Its new versions were defined in 1999 and 2008. The latest version of FRAME is aligned with the methodology on which the European norms defining machine safety EN 954-1 and EN 14121-1:2007 are based, which were revised and published in 2010 as ISO 12100:2010.

The second group of procedures aims to assess the minimum necessary fire resistance of building structures. The first was developed by Gellinger in 1950 for industrial buildings with metal structures. His procedure was expanded by German engineer Halpap for other industrial buildings. Halpap's procedure was standardized in 1964 in the form of the DIN18230 standard. In our country, this standard was translated as SRPS TR19:1997. New versions of the DIN18230 standard (with expanded tables) were published in 1998 and 2010. In 2012, the SRPS-EN199 1-1-2:2012 standard was adopted, in which Halpap's calculation procedure was modified. The PURT-EUROALARM method was applied to assess the fire risk for a hazardous materials warehouse and define protection measures to proactively improve the fire protection system.

2. METHODS

The fire risk assessment was carried out using the PURT-EUROALARM method, which pertains to the calculation of the fire risk of the building and the fire risk of the building's contents. The PURT-EUROALARM method, though named after its creator, is occasionally referred to by the name of the institution where he was employed—the European Association of Fire Alarm Manufacturers. This method evaluates fire risk by assessing 10 Fire Vulnerability Components, which consider factors such as the susceptibility of structural materials, the impact of smoke, the occupants' vulnerability, and the effectiveness of fire suppression systems [16].

The data related to the fire risk calculation for the hazardous materials warehouse are approximate and based on empirical knowledge.

3. RESULTS AND DISCUSSIONS

The raw materials used in the technological process are stored in a hazardous materials warehouse and are then pumped through a closed pipe system into production. The materials used are mainly organic solvents (Petroleum benzine 60-95, Phenol/Cressol and others). Accordingly, a fire risk assessment for the hazardous materials warehouse has been carried out, based on the intensity and duration of the fire, as well as on the structural characteristics of the building's load-bearing elements, according to Equation 1.

$$R_0 = \frac{(P_0 \times C + P_k) \times B \times L \times S}{W \times R_i} \tag{1}$$

Where is:
R_0 - fire risk of the warehouse;
P_0 - fire load coefficient of the warehouse contents;
C - combustibility coefficient of the warehouse contents;
P_k - fire load coefficient of the materials used in the warehouse construction;
B - size and position coefficient of the fire sector;
L - delay coefficient of the firefighting start;
S - width coefficient of the fire sector;
W - fire resistance coefficient of the warehouse's load-bearing structure;
R_i - risk reduction coefficient.

The fire load coefficient of the warehouse contents (P_0) is determined based on the heat value of all combustible materials in the warehouse in MJ/m², as shown in the following Table 1.

Table 1 Fire load coefficient of warehouse contents (P_0)

MJ/m²	0 - 251	252 - 502	503 - 1004	1005 - 2009	2010 - 4019	4020 - 8038	8039 - 16077	16078 - 32154	32155 - 64309	≥64310
P_0	1	1.2	1.4	1.6	2.0	2.4	2.8	3.4	3.9	4.0

If the calculated total heat value of all combustible materials in the warehouse is 4500 MJ/m², it follows from Table 1 that the coefficient P_0 is 2.4.

The combustibility coefficient (C) is determined according to the fire hazard class, as shown in Table 2.

Table 2 Combustibility coefficient of the warehouse contents (C)

Fire hazard class	VI	V	IV	III	II	I
Combustibility coefficient (C)	1.0	1.0	1.0	1.2	1.4	1.6

The hazardous materials warehouse falls into fire hazard class III. From Table 2, it follows that the combustibility coefficient (C) is 1.2.

The fire load coefficient of the warehouse construction (P_k) is determined based on the heat value of all combustible materials in the building in MJ/m², as shown in Table 3.

Table 3 Fire load coefficient (P_k)

MJ/m²	0-419	420-837	838-1675	1676-4187	≥4188
P_k	0	0.2	0.4	0.6	0.8

The calculated total heat value of all combustible materials in the warehouse is 2500 MJ/m². From Table 3, it follows that the fire load coefficient of the warehouse construction (P_k) is 0.6.

The coefficient of the size and position of the fire sector (B) is determined according to the descriptive characteristics of the warehouse, as shown in Table 4.

Table 4 Size and position coefficient of the fire sector (B)

Characteristics of the building	Fire sector up to 1500 m², room height up to 10 m, a maximum of 3 floors	Fire sector from 1500 to 3000 m², room height from 10 to 25 m, one floor in the basement	Fire sector from 3000 to 10,000 m², room height over 25 m, 2 or more floors in the basement	Fire sector over 10,000 m²
B	1.0	1.3	1.6	2.0

According to the description of the warehouse characteristics from Table 4, the coefficient B is 1.

The delay coefficient for the start of the intervention (L) depends on the equipment and type of fire brigade intervening, as well as its distance from the building, as shown in Table 5.

Table 5 Delay coefficient of the firefighting start (L)

Time until the start of firefighting Distance of the fire brigade		10' 1 km	10'-20' 1-6 km	20'-30' 1 km	≥30' 1-6 km
Type of fire brigade	Professional industrial fire brigade	1.0	1.1	1.3	1.5
	Volunteer industrial fire brigade	1.1	1.2	1.4	1.6
	Territorial professional fire brigade	1.0	1.1	1.2	1.4
	Territorial volunteer fire brigade with permanent duty	1.1	1.2	1.3	1.5
	Territorial volunteer fire brigade without permanent duty	1.3	1.4	1.6	1.8

Based on the optimal time to start firefighting and the distance of the fire brigade from the building, Table 5 indicates that the coefficient L is 1.

The width coefficient (S) depends on the width of the fire sector, as shown in Table 6.

Table 6 Width coefficient of the fire sector (S)

Minimum width of the fire sector [m]	< 20	20-40	40-60	≥60
S	1	1.1	1.2	1.3

Based on the width of the fire sector, Table 6 indicates that the coefficient S is 1.

The fire resistance coefficient (W) of the load-bearing structure depends on the structural characteristics of the building, as shown in Table 7.

Table 7 Fire resistance coefficient of the warehouse's load-bearing structure (W)

Fire resistance in minutes	< 30	30	60	90	120	180	240
Fire resistance coefficient (W)	1.0	1.3	1.5	1.6	1.8	1.9	2.0

Based on the structural characteristics of the building, Table 7 indicates that the fire resistance coefficient W is 1.8.

The risk factor coefficient (Ri) is calculated considering the type of combustible material, storage method, burning rate, and other influencing factors. The fire risk of the building can be reduced depending on the risk factor coefficient, with values provided in Table 8.

Table 8 Risk reduction coefficient (R_i)

Risk	Circumstances affecting the risk assessment	Ri
Maximum	High flammability of materials and storage with larger clearances; expected rapid spread of fire; presence of a higher number of potential ignition sources in the technological process or during storage	1.0
Normal	Flammability is not excessively high, and storage has sufficient clearances for handling; normal rate of fire spread is expected; normal ignition sources are present in the technological process or during storage	1.3
Less than normal	Lower flammability due to partial storage (20-25%) of combustible goods in non-combustible packaging; storage of combustible goods without clearances; rapid spread of fire is not expected; for ground-level halls with an area less than 3000 m^2; for buildings where smoke and heat extraction is adequately managed	1.6
Negligible	Low probability of ignition due to goods stored in metal crates or similar materials, as well as very dense storage; very slow fire development is expected	2.0

Based on the type, storage method, and combustion rate of combustible materials, it follows from Table 8 that the coefficient R_i is 1.

Considering the parameters that have been presented the fire risk calculation for the hazardous materials warehouse is:

$$R_0 = \frac{(2.4\times1.2+0.6)\times1\times1\times1.2}{1.8\times1} = 2.32 \quad (2)$$

The fire risk of the building's contents depends on the potential danger to people, equipment, furniture, stored goods, etc., and is calculated using the following formula:

$$R_s = H \times D \times F \quad (3)$$

Explanation of the formula:
R_s - Fire risk of the building's contents;
H - Coefficient of danger to people;
D - Property risk coefficient;
F - Smoke impact coefficient.

The coefficient of danger to people (H) depends on the possibility of timely evacuation of people from the building and is determined as shown in Table 9.

Table 9 Coefficient of danger to people (H)

Degree of threat	Coefficient of danger to people (H)
There is no danger to the person	1.0
There is danger for people, but they can save themselves	2.0
There is a danger to people, and evacuation is difficult (heavy smoke, a large number of people present, a multi-storey building, rapid fire development, the presence of immobile persons - sick, children, elderly)	3.0

Based on the level of threat and the possibility of timely evacuation of people from the building, it follows from Table 9 that the coefficient H is 2.

The property risk coefficient (D) depends on the concentration of value within a single fire sector, as well as the possibility of replacing the destroyed property, as shown in Table 10.

Table 10 Property risk coefficient (D)

Concentration of value	Property risk coefficient (D)
The contents of the building do not represent significant value or are not highly susceptible to destruction	1.0
The contents of the building have value and are susceptible to destruction	2.0
The destruction of value is definitive and the loss is irreplaceable (such as cultural assets, etc.), or the destruction indirectly threatens the livelihood of the population	3.0

Based on the concentration of value and the possibility of replacing the destroyed property of the building, it follows from the table that the coefficient D is 2.

The presence of a large amount of smoke increases the risk to people and property (due to its toxic and corrosive nature) and is taken into account through the smoke impact coefficient (F), as shown in Table 11.

Table 11 Smoke impact coefficient (F)

Circumstances leading to smoke inhalation	F
There is no particular risk of fumes and corrosion	1.0
More than 20% of the total weight of all fuels causes smoke or emit toxic combustion products	1.5
More than 50% of the substances present generate smoke or emit toxic combustion products or more than 20% consist of substances present that emit highly corrosive gases	2.0

Based on the description of circumstances leading to smoke and/or corrosion, it follows from Table 11 that the coefficient F is 1.5.

According to the adopted values, the fire risk of the building's contents is calculated using the formula:

$$R_s = 2 \times 2 \times 1.5 = 6 \quad (4)$$

Since all circumstances and data about the building have been considered for calculating R_0 and R_S through the coefficients, the required type of protection for the hazardous materials warehouse can be determined according to the decision diagram. By applying the obtained values of R_0 and R_S to the diagram, it is possible to determine what type of protection should be implemented for the building, as illustrated in Figure 1.

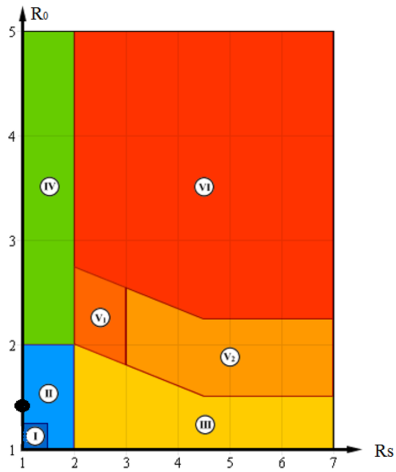

Fig. 1 Decision diagram

Explanatory diagram:
I preventive measures are sufficient
II fire alarm and extinguishing systems are not required
III alarm system is required but not a fire extinguishing system
IV extinguishing system is required but not a fire alarm system
V_1 fire extinguishing system is required
V_2 fire alarm system is required
VI fire extinguishing and warning systems are needed

Considering that the value of R_0 is 2.32 and the value of R_S is 6, the fire risk in the hazardous materials warehouse falls into group V_2, which necessitates the installation of a fire alarm system.

Hazardous chemical leaks from storage equipment can lead to fire and explosion accidents if the chemicals come into contact with an ignition source. To enhance risk control measures and prevent the escalation of such accidents, researchers globally have studied the occurrence, progression, and characteristics of fires at different stages. Wu et al. introduced an innovative fire detection method using video cameras, where a machine-learning algorithm creates a fire detection model. This system can detect fires and export the coordinates of the fire area upon capture [17]. Cheng and Hadjisophocleous developed a dynamic model that accounts for both horizontal and vertical fire spread, applicable to all building types and beneficial for fire risk assessment in building safety design [18]. Additionally, a model for analyzing the probability of fire accidents was proposed, emphasizing the significance of time-dependent fire scenarios, which was utilized for time-based fire probability analysis and system optimization [19]. Ding et al. created a comprehensive framework for the quantitative risk management of warehouse fires by examining past incidents and suggesting specific safety measures [20]. Accordingly, a fire protection system based on fire detection predicts the development of a fire and the implementation of the best preventive technical and organizational protection measures.

4. Conclusion

The assessment of fire risks in a warehouse that stores hazardous materials has been conducted thoroughly by evaluating the fire risk coefficients R_0 and R_S based on the specific circumstances and data related to the building. The analysis revealed that the value of R_0 is 2.32 and R_S is 6, which places the fire risk in the warehouse within group V_2. This classification indicates a high level of fire risk due to the nature of the stored materials and the potential impact on safety. As a result, it is evident that the warehouse requires a robust fire protection system. Specifically, the implementation of a fire alarm system is necessary to ensure timely detection and response in the event of a fire. This measure will significantly enhance the safety of the facility, mitigate potential damage, and protect both personnel and property from fire hazards. In conclusion, addressing the identified fire risks with appropriate protective measures will contribute to a safer working environment and ensure compliance with fire safety regulations. It is recommended that the warehouse management prioritize the installation and maintenance of the recommended fire protection systems to effectively manage and reduce fire risks.

Acknowledgement: *This paper is a part of the research funded by the Ministry of Education, Science and Technological Development of the Republic of Serbia pursuant to agreement No. 451-03-66/2024-03/ 200148.*

REFERENCES

1. Ерић М. (2003). *Противпожарна и превентивно-техничка заштита*, Издавач:"Јел&Мил" Чачак
2. Pheng L.S, Raphael B, Kit W.K. (2006). *Tsunamis: some pre-emptive disaster planning and management issues for consideration by the construction industry*, Structural Survey, 24, pp. 378-396
3. Khorram-Manesh A. (2017). *Handbook of Disaster and Emergency Management*
4. Alexander D. (2019). L'Aquila, *Central Italy, and the „disaster Cycle", 2009-2017*, Disaster Prevention and Management
5. Sawalha I.H. (2020). *A contemporary perspective on the disaster management cycle*, Foresight, 22, pp. 469-482
6. Martinson E.J, Omi P.N. (2003). *Performance of Fuel Treatments Subjected to Wildfires*, USDA Forest Service - Research Paper, RMRS-RP, pp. 1-38
7. Piñol J, Castellnou M, Beven K.J. (2007). *Conditioning uncertainty in ecological models: assessing the impact of fire management strategies*, Ecological Modelling, 207, pp. 34-44
8. Higgins E, Taylor M, Francis H. (2012). *A systemic approach to fire prevention support*, Systemic Practice and Action Research, 25, pp. 393-406
9. MPSS, Fire Safety Policy Basic Plan. (2016). *Public Safety and Security*
10. Shoaf K.I, Rottman S.J. (2000). *The role of public health in disaster preparedness, mitigation, response, and recovery*, Prehospital and Disaster Medicine, 15, pp. 18-20
11. Wuschke K, Clare J, Garis L. (2013). *Temporal and geographic clustering of residential structure fires: a theoretical platform for targeted fire prevention*, Fire Safety Journal, 62, pp. 3-12
12. Jonsson A, Runefors M. S¨ardqvist S, Nilson F (2016). *Fire-related mortality in Sweden: temporal trends 1952 to 2013*, Fire Technology, 52, pp. 1697-1707
13. Taylor M, Appleton D, Keen G, Fielding J.(2019). *Assessing the effectiveness of fire prevention strategies*, Public Money & Management, 39, pp. 418-427
14. Eric Dickson T.A, Baker J.L, Hoornweg D. (2012). *Urban Risk Assessments: Understanding Disaster and Climate Risk in Cities*, Washington, DC: World Bank
15. Аранђеловић И, Рајић Р, Савановић Марко. (2017). *Поступци за процену ризика од пожара*. Процесна техника, 29, пп. 24-28
16. Purt G.A. (1972). *The evaluation of the fire risk as a basis for planning automatic fire protection systems*, Fire Technology, 8, pp. 291-300
17. Wu H, Wu D, Zhao J. (2019). An intelligent fire detection approach through cameras based on computer vision methods. Process Safety and Environmental Protection, 127, pp. 245-256
18. Cheng H, Hadjisophocleous G.V. (2011). *Dynamic modeling of fire spread in building*, Fire Safety Journal, 46, pp. 211-224
19. Yang X, Li Y, Chen Y, Li Duh Y.S.(2020). *Case study on the catastrophic explosion of a chemical plant for production of m-phenylenediamine[J]*. Journal of Loss Prevention in the Process Industries, 67
20. Ding L, Khan F, Ji J. (2020). *Risk-based safety measure allocation to prevent and mitigate storage fire hazards*. Process Safety and Environmental Protection. 135, 282-293

PROCENA POŽARNOG RIZIKA SKLADIŠTA OPASNIH MATERIJA

Zaštita od požara u skladištima opasnih materija temelji se na detaljnoj analizi relevantnih parametara koji se odnose na požarni rizik objekta i uskladištenog materijala kako bi se utvrdile odgovarajuće mere zaštite od požara. Ovaj rad analizira potencijalne opasnosti koje se javljaju pri skladištenju opasnih materija i procenjuje rizik nastanka požara. Analizirani su faktori koji doprinose povećavanju rizika od požara, kao što su zapaljivost materijala, uslovi skladištenja i postojeće mere zaštite. Cilj rada je identifikovati ključne parametre koji mogu uticati na nastanak požara u skladištima opasnih materija i u skladu sa tim definisati stepen zaštite od požara.

Ključne reči: *rizik nastanka požara, procena rizika, skladište opasnih materija.*

FACTA UNIVERSITATIS
Series: **Working and Living Environmental Protection** Vol. 21, Nº 2, 2024, pp. 119 - 131
https://doi.org/10.22190/FUWLEP240904011D

Original Scientific Paper

THE INFLUENCE OF SAFETY DIODES ON THE CHARACTERISTICS OF THE PHOTOVOLTAIC PANELS UNDER NON-UNIFORM ENVIRONMENTAL CONDITIONS

UDC 621.382:541.13

Marko A. Dimitrijević, Milutin P. Petronijević

Faculty of Electronic Engineering, University of Niš, Serbia

ORCID iDs: Marko A. Dimitrijević https://orcid.org/0000-0001-9032-9595
Milutin P. Petronijević https://orcid.org/0000-0003-2396-0891

Abstract. *The operation of photovoltaic systems depends on the environmental conditions, which affect the current-voltage characteristics of photovoltaic modules and more complex structures. Under non-uniform environmental conditions - different illumination of cells within one module - the characteristics of the module can be increasingly complex. Safety bypass diodes, which are connected in parallel with the cells and protect them from overheating during partial shading, also contribute to this complexity. In order to evaluate the performance of the photovoltaic system, specifically the inverter and the algorithm for maximum power point tracking, it is necessary to take into account these influences on the characteristics of the photovoltaic structures. In this manuscript, the influence of illumination and temperature on individual photovoltaic cells, the topology of a photovoltaic module including bypass diodes, as well as the characteristics of modules with protective bypass diodes under non-uniform environmental conditions are discussed.*

Key words: *photovoltaic cell, photovoltaic module, bypass diodes, current-voltage characteristics*

1. INTRODUCTION

The climate has undergone significant changes in the past hundred years [1], mostly caused by anthropogenic factors. Some of the most significant changes are global warming, ocean acidification, and changes in ecosystems. The Earth's average surface temperature has increased by approximately 1.2°C since the end of the 19th century. Most of the warming has occurred in the past four decades. The oceans have absorbed much of this increased heat, with a temperature rise of more than 0.2°C in half of a century. The direct consequences of global warming are shrinking ice sheets, glacial

Received September 4, 2024 / Accepted October 11, 2024
Corresponding author: Marko A. Dimitrijević
Faculty of Electronic Engineering, Aleksandra Medvedeva 4, 18000 Niš, Serbia
E-mail: marko@venus.elfak.ni.ac.rs

retreat and decreased snow cover. The acidity of surface ocean waters has increased by about 26% since the beginning of the Industrial Revolution [2, 3]. Global sea level has risen about 21cm since the beginning of the 20th century. The rate in the last two decades, however, is nearly double that of the last century and is accelerating slightly every year [4].

Climate change has a direct impact on changes in wildlife and ecosystems [5]. Many species are shifting their geographic ranges, seasonal activities, migration patterns, and interactions with other species in response to climate change. Indirectly or directly, it also affects human lives. We are witnessing an increase in the frequency and intensity of extreme weather events, including heatwaves, heavy rainfall, droughts, and hurricanes [6]. Denying climate change is increasingly meaningless.

These changes are largely attributed to increased concentrations of greenhouse gases, such as carbon dioxide (CO_2), methane (CH_4), and nitrous oxide (N_2O), resulting from human activities: mostly burning fossil fuels, deforestation, and industrial development.

With the growing awareness of global climate change, efforts to reduce it have also intensified. As these changes are mainly caused by the ever-increasing need for energy production and the consequently enormous use of fossil fuels, most efforts have been made to find new, cleaner energy sources. In response to these challenges, the global and mass usage of photovoltaic technologies began at the beginning of the century. In 2023 alone, the total capacity of solar power plants installed around the planet has increased by 410GW, which is almost half of the previously installed capacity [7].

A large share of the total photovoltaic capacity comprises residential systems connected to the power grid [8]. One such system consists of a photovoltaic (PV) array, DC to AC converter – PV inverter, and optional energy storage – battery. The PV inverter is equipped with a controller whose function is to determine the maximum power operating point of the PV array. The controller achieves this by executing the Maximum Power Point Tracking (MPPT) algorithm. There are several implementations of the MPPT algorithm, a detailed description of their implementations and characteristics is described in [9-11].

The basic photovoltaic component is the photovoltaic cell [12]. The voltage generated by the cell is between 0.5V and 0.6V. To achieve the appropriate voltage for conversion, multiple cells are connected in a photovoltaic module (panel) with a series connection, and the modules are connected in series in a photovoltaic string [13]. Finally, multiple strings are connected in parallel or in series in a structure called a photovoltaic array to generate the necessary DC power.

The current-voltage (I-V) characteristic of the PV array will depend on the characteristics of the individual cells, as well as the way they are connected into modules, i.e. strings and arrays. If the array is formed from modules with the same characteristics, and if all modules work under the same, uniform environmental conditions (illumination, temperature), the shape of the I-V characteristic of the array will have the same shape as the characteristic of the individual cell. However, in real (non-uniform) environmental conditions, the I-V characteristics of the cells will be different, and the resulting characteristic of the entire array will be more complex. Moreover, PV modules contain safety diodes that affect the equivalent characteristics.

Operation of the PV inverter, i.e. conversion of DC to AC voltage, more precisely the maximum achievable power depends on the characteristic of the array to which it is connected. Knowing the shape of the PV array characteristic, as well as its dependence on array topology and environmental conditions, is therefore important.

This paper will summarize the operation mode of the PV cell and PV module, with special reference to the operation in non-uniform conditions. The function of safety diodes will be explained, as well as their influence on the characteristics of PV modules. The characteristics of more complex PV structures can be derived based on the characteristics of the modules and how they are connected.

The manuscript is organized as follows: Section 2 presents the operation of the photovoltaic cell, its most used single-diode model, and the equation that describes the current-voltage characteristic of the cell based on the given model. Also, the dependence of the characteristics on environmental conditions, specifically illumination and temperature, was elaborated. Section 3 describes the PV module, and its operation under uniform environmental conditions and under partial shading, i.e. different cell illumination. Finally, the function of safety diodes is presented and their influence on the I-V characteristic of the module is discussed in detail. Section 4 concludes the manuscript.

2. The Characteristics of PV Cell

A photovoltaic (PV) cell is a semiconductor device that converts visible or near-visible electromagnetic radiation into electricity through the photovoltaic effect. Photovoltaic power plants are complex structures that are essentially formed by connecting a large number of photovoltaic cells. The characteristics of these structures depend on the characteristics of the individual cells from which they are made, as well as on the topology, i.e. how the cells are interconnected.

The PV cell is implemented as a semiconductor p-n junction. The p-n junction represents the basic semiconductor structure, which is made by doping the semiconductor with different types of dopants. One part of the junction is a p-type semiconductor, made by doping with acceptors, dopants of the third group of elements of the periodic table, such as boron. The second part of the junction is an n-type semiconductor, made by doping with donors, elements of the fifth group of elements, such as phosphorus.

2.1. The Single-diode model of PV cell

There are several PV cell models, highlighting different cell properties. Most models are static, and are used to model cells in DC operation. In [14, 15] the dynamic characteristics of the PV cell are presented. The simplest static cell model is the single-diode model, which is the most widely used because of its simplicity [16]. In further consideration, for the analysis of static current-voltage (I-V) and power-voltage (P-V) characteristics, this model will be used (Fig 1).

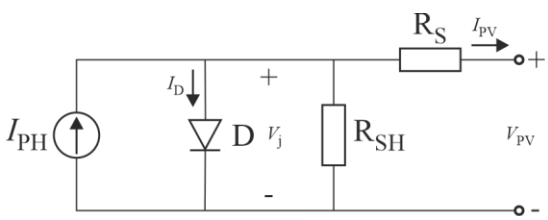

Fig. 1 Singe-diode model of PV cell. R_S is the series resistance, R_{SH} is the parallel

(shunt) resistance of the model.

The dependence of cell current I_{PV} on cell voltage V_{PV} defines the current-voltage characteristic of a PV cell. This dependence, based on the single-diode model shown in Fig. 1, can be represented by the equation:

$$I_{PV} = I_{PH} - I_S\left(e^{\frac{q_e(V_{PV}+I_{PV}R_S)}{nkT}} - 1\right) - \frac{V_{PV}+I_{PV}R_S}{R_{SH}}, \quad (1)$$

where I_{PH} represents photocurrent, I_S is the reverse saturation current of a p-n junction, $q_e$stands for the electron charge (1.6×10^{-19}C), k is the Boltzmann constant (1.38×10^{-23} J/K), T is cell absolute temperature (K), and n is the diode ideality factor.

The single-diode model can be further simplified if the series ($R_S = 0$) and parallel ($R_{SH} = \infty$) resistances of the model are neglected.

The equation **Error! Reference source not found.** is a non-linear equation, and the current I_{PV} figures are on both sides of the equation. Furthermore, I_{PV} exists in both the linear term and the exponent on the left-hand side of the equation. However, by applying the Lambert W-function [17], it is possible to obtain an explicit current-voltage dependence of the PV cell [18]:

$$I_{PV} = \frac{I_{PH}+I_S-V_{PV}/R_{SH}}{1+R_S/R_{SH}} - \frac{nV_T}{R_S}W\left(\frac{I_S R_S}{nV_T(1+R_S/R_{SH})}e^{\frac{V_{PV}}{nV_T}\left(1-\frac{R_S}{R_S+R_{SH}}\right)+\frac{(I_{PH}+I_S)R_S}{nV_T(1+R_S/R_{SH})}}\right), \quad (2)$$

where $V_T = \frac{kT}{q_e}$ represents thermal voltage.

2.2. The current-voltage characteristics

The current-voltage (I-V) characteristic of the PV cell, for $I_{PH} = 8.24$A, $I_S = 2.36$nA, $R_{SH} = 1000\Omega$, $R_S = 0.002\Omega$, $n = 1.3$ and at temperature $T = 298$K is shown in Fig. 2. The characteristic is obtained by means of simulation, using *pvlib* library for Python [19].

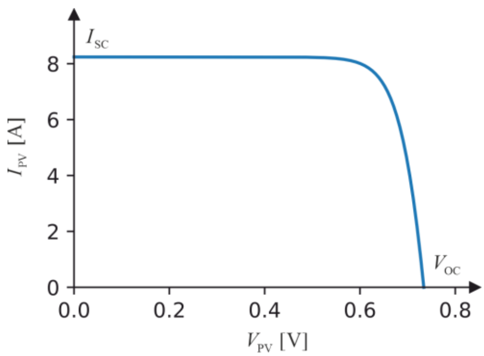

Fig. 2 The current-voltage characteristic of PV cell. I_{SC} represents the short-circuit current and V_{OC} is the open-circuit voltage of the PV cell.

Two terminal points can be observed on the characteristic, the first is a short-circuit of the PV cell ($I_{PV} = I_{SC}$, $V_{PV} = 0$) and the second is an open-circuit ($I_{PV} = 0$, $V_{PV} = V_{OC}$). If the resistances in the single-diode model are ignored, according to the equation **Error! Reference source not found.**, approximate values for the short-circuit current and open-circuit voltage can be calculated as:

$$I_{SC} \approx I_{PH}, \tag{3}$$

$$V_{OC} \approx \frac{nkT}{q_e} \ln\left(\frac{I_{PH}}{I_S} + 1\right). \tag{4}$$

2.3. The temperature and illumination dependence

The characteristic of the PV cell depends on the environmental conditions, i.e. illumination and temperature. In addition to the explicit temperature dependence, which can be observed in the equation **Error! Reference source not found.**, other parameters also depend on environmental conditions. The reverse saturation current of the p-n junction has a complex dependence on temperature [20]:

$$I_S \sim T^{\frac{3}{n}} e^{\frac{E_g}{nkT}} \tag{5}$$

where E_g is the band-gap of the cell material (1.12eV for silicon).

The dependence of the photocurrent on temperature T and illumination G is approximately linear, therefore an empirical formula is used for its Anderson translation model [21]:

$$I_{PH} = (I_{STC} - \beta(T - T_{ref})) \cdot \frac{G}{G_{ref}} \tag{6}$$

where I_{STC} is short-circuit current under standard testing conditions, defined with T_{ref} = 298K and G_{ref} = 1000W/m^2, and β represents the current temperature coefficient (A/K). The illumination and temperature dependencies of the I-V characteristic of the PV cell are shown in Fig. 3.

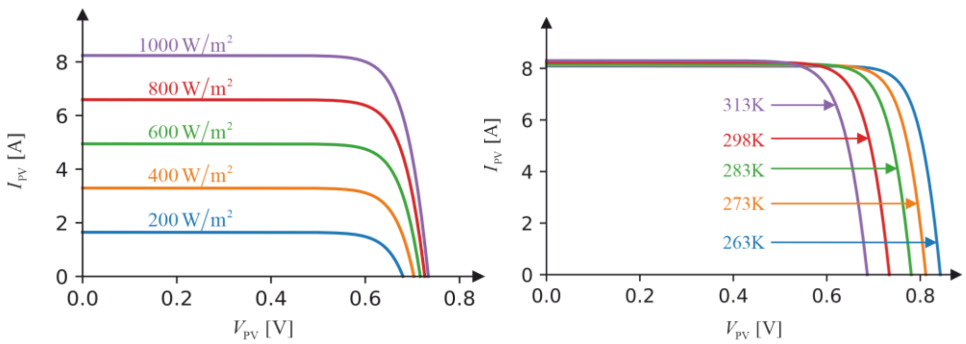

Fig. 3 The PV cell characteristics for different illuminances, from 200 W/m^2 to 1000 W/m^2 at the same temperature, T_{ref} = 298K (left) and for different temperatures, from 263K to 313K at the same illumination, G_{ref} = 1000W/m^2 (right).

3. PHOTOVOLTAIC MODULE

3.1. Photovoltaic module under uniform illumination

Photovoltaic (PV) modules are monolithic structures made by a series of connections of cells implemented in the same technology. Therefore, the I-V characteristics of all cells within one module are almost identical under uniform illumination and temperature of the module. In this case, the equivalent module I-V characteristic can be calculated according to the Kirchoff voltage law (KVL). As the cells are connected in series, the current flowing through each cell is the same and it is also the output current of the module. According to KVL, the output voltage of the module is equal to the sum of the cell voltages. The equivalent I-V characteristic of a module resembles the shape of individual cell characteristics, with identical current and voltage multiplied by the number of cells in the module (Fig. 4, left). The power-voltage (P-V) characteristic, the power dependence on the voltage of the module under conditions of uniform illumination has one maximum – maximum power point (Fig. 4, right).

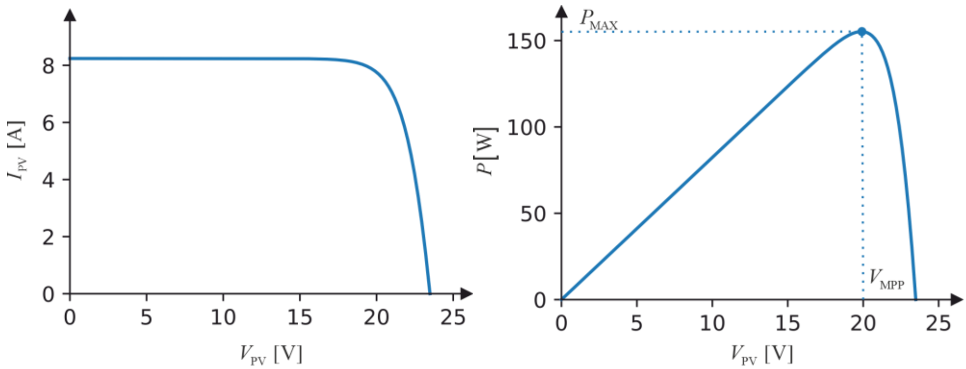

Fig. 4 I-V characteristic of PV module (left) and P-V characteristic (right). Maximal power is achieved for maximum power point voltage V_{MPP}.

3.2. Photovoltaic module under nonuniform illumination

However, in real exploitation, individual cells within the module may be shaded, soiled, or heated differently. Thus, cells under different conditions have different short-circuit current and open-circuit voltage, hence different I-V characteristics in general. In order to analyse the operation of a PV module under such nonuniform environmental conditions, the equivalent circuit of a series connection of differently illuminated cells is used as a simple model, shown in Fig. 5.

For the sake of simplicity, a single-diode model with $R_S = 0$ and $R_{SH} = \infty$ is used. One cell in a series connection is shaded, producing photocurrent I_{PH2}, and other n cells are fully illuminated, generating I_{PH1}. The short-circuit current of the described topology is limited to the smallest photocurrent in serial connection, i.e. to the photocurrent of the most shaded cell. According to KVL, the voltage of a shaded cell is negative:

$$V_{j2} = -nV_{j1} \tag{7}$$

and the p-n junction of this cell is reverse-biased.

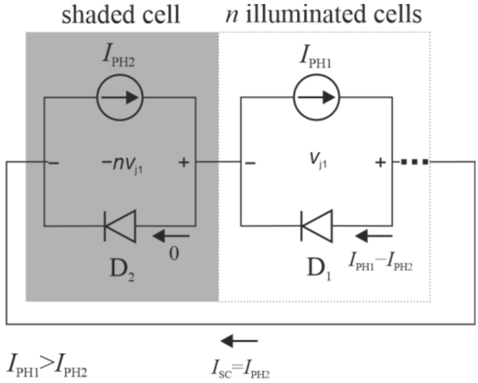

Fig. 5 The series connection of PV cells, one cell is shaded and n cells are fully illuminated. The shaded cell has a smaller photocurrent and limits module current. Furthermore, considerable power is dissipated, leading to the appearance of hot spots and potential damage or destruction.

When a module is short-circuited, considerable power is dissipated on the shaded cell, which can lead to its overheating, the appearance of hot spots on the module, and potential damage.

3.3. The bypass diodes

Dissipation can be reduced by connecting safety diodes - bypass diodes D_{BP} in parallel to the shaded cells, Fig. 6, protecting them from overheating and damage.

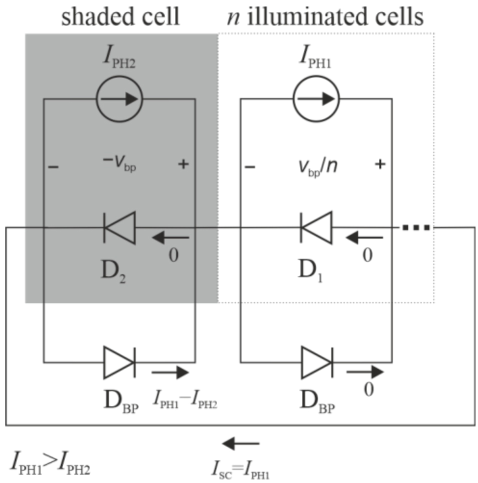

Fig. 6 The bypass diodes connected in parallel to cells.

The bypass diode is connected in opposite polarity to the p-n junction of the cell. When a negative voltage appears due to cell shading, the bypass diode is forward-biased.

The voltage of the shaded cell is equal to forward forward-biased bypass diode p-n junction voltage drop:

$$V_{j2} = -V_{bp}, \tag{8}$$

which is significantly less than in the case without the connected bypass diode. Consequently, the dissipated power on the shaded cell is approximately n times smaller. The bypass diode current is equal to the difference between fully illuminated cell photocurrent and shaded cell photocurrent:

$$I_{bp} = I_{PH1} - I_{PH2}. \tag{9}$$

The short-circuit current of a series connection I_{SC} in this case is equal to a fully illuminated cell photocurrent, I_{PH1}.

The I-V characteristic, determined by the current I_M, of a module containing shaded cells can be calculated using equivalent circuits, shown in Fig. 7 and Fig. 8. If the module is loaded with high resistance, the current of the module, i.e. the series connections of the cells will be less than the photocurrents: $I_{PH1} > I_{PH2} > I_M > 0$. This case is illustrated in Fig. 7.

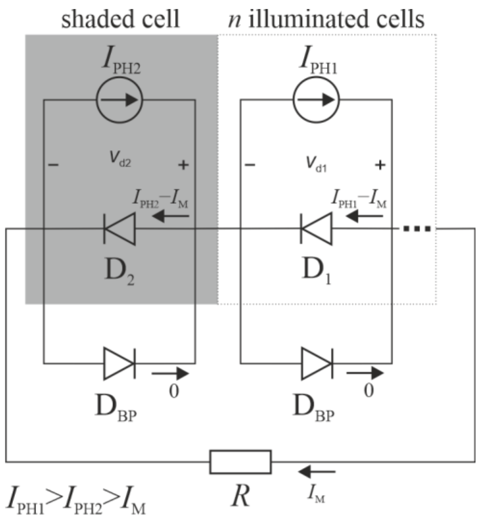

Fig .7 The PV module loaded with high resistance, corresponding to $I_{PH1} > I_{PH2} > I_M > 0$.

The p-n junctions of all the cells within the module are forward-biased and the bypass diodes are reverse-biased so that the total voltage of the module is equal to the sum of the voltages of the individual cells:

$$V_M = V_{j2} + nV_{j1} \tag{10}$$

For $I_{PH1} > I_{PH2} > I_M$, equivalent characteristics can be modelled by summing the cell voltages for the equal cell currents.

The circuit depicted in Fig. 8 corresponds to a low load resistance when the module current is greater than the shaded cell photocurrent, $I_{PH1} > I_M > I_{PH2}$.

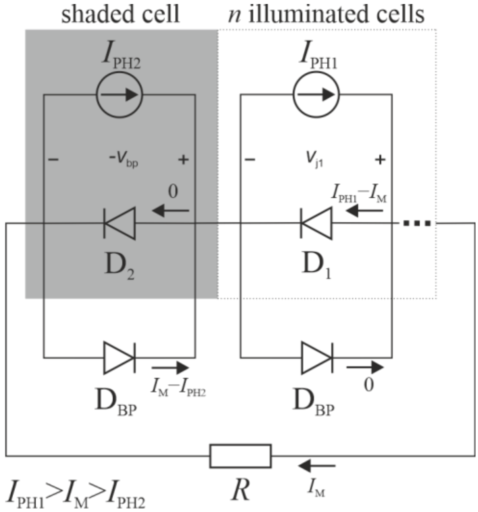

Fig. 8 The PV module loaded with low resistance, corresponding to $I_{PH1} > I_M > I_{PH2}$.

In this configuration, only the p-n junctions of the illuminated cells are forward-biased. The p-n junction of the shaded cell is reverse-biased, and the diode bypassing this cell is forward-biased. The voltage of the module is:

$$V_M = -V_{bp} + nV_{j1}. \tag{11}$$

For $I_{PH1} > I_M > I_{PH2}$, the equivalent characteristic of a module can be modelled by summing only voltages of the fully illuminating cells for the equal currents, and subtracting voltage drop on forward biased bypass diodes.

The previous consideration can be generalized to cases where there are multiple equally shaded cells, or when the illumination of the cells in the module is different.

3.2. Practical implementations of PV modules

In commercial modules, for practical reasons, one bypass diode is connected in parallel with multiple cells. An example of this topology is illustrated in Fig. 9. The module consists of 12 cells connected in series, in such a manner that groups of four cells are protected by one bypass diode. One cell is shaded, and it generates a photocurrent I_{PH2}. Other cells are fully illuminated, generating I_{PH1}. The case where $I_{PH1} > I_M > I_{PH2}$ is illustrated. The p-n junction of the shaded cell is reverse-biased, and the cell voltage is

$$V_{j2} = -V_{bp} - 3V_{j1} \tag{12}$$

which is a four times higher voltage than in the case when each cell is protected by a bypass diode, but still three times less than in the case when the bypass diodes are not connected. When designing a PV module, it is necessary to take into account the maximum power that can be dissipated on the cell, so that damage does not occur. Based on the maximum dissipation and photocurrent at maximum illumination, the optimal number of cells that can be protected by one bypass diode can be determined.

For the given example, the module output voltage is:

$$V_M = -V_{bp} + 8V_{j1}. \quad (13)$$

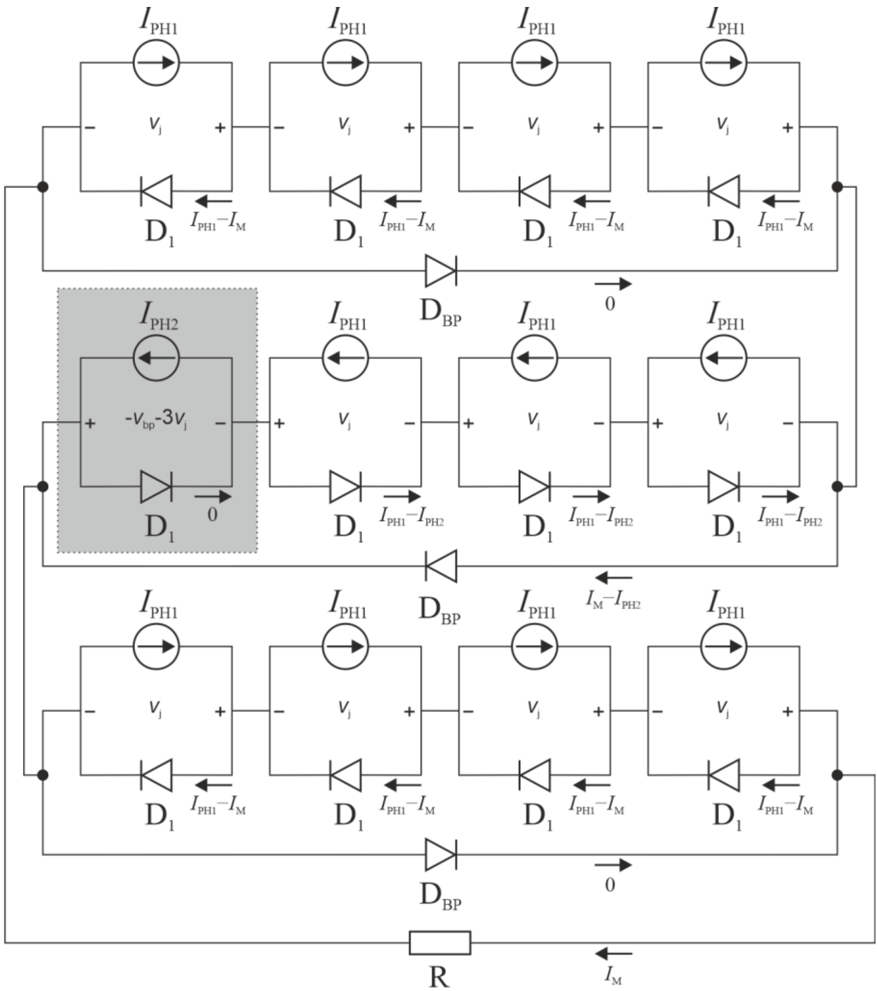

Fig. 9 The PV module with 12 cells, protected with 3 bypass diodes.

3.4. The I-V and P-V characteristics of partially shaded PV module

Based on the previous analysis, it is possible to calculate the I-V and P-V characteristics of a partially shaded PV module based on the known characteristics of individual PV cells for a given illumination.

The example of I-V and P-V characteristics of a PV module under partial shading is shown in Fig. 10. The characteristics shown corresponds to a PV module with 30 cells, of which 24 are fully illuminated, $G = 1000\text{W/m}^2$, while 6 cells are shaded, with $G = 600\text{W/m}^2$. The temperature of all cells is $T_{ref} = 298\text{K}$.

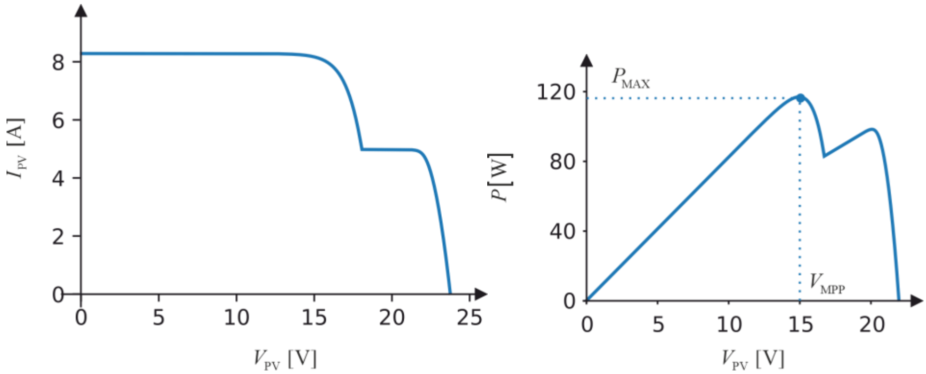

Fig. 10 The simulated I-V and P-V characteristics of the PV module.

The P-V characteristic of partially shaded modules exhibits multiple local maxima, corresponding to different module voltages. The largest of all local maxima is the global maximum – maximum power point P_{MAX}, determined by the voltage V_{MPP}.

4. Conclusion

Knowing the I-V and P-V characteristics of the PV module under non-uniform environmental conditions, such as different illumination or temperature of individual cells in the module, is necessary to evaluate the performance of photovoltaic converters operating in real climatic conditions [22]. Those characteristics, as well as characteristics of more complex structures such as strings and arrays, can be increasingly complex depending on the connection of bypass diodes, the topology of the entire PV structure and the shading pattern. The most significant manifestation of this complexity can be observed on the P-V characteristic, in the form of multiple local maxima, which can mislead the MPPT algorithm. For example, many commercial inverters will, in the case of a characteristic similar to the one shown in Fig. 10, select the operating point at the local maximum that is closest to the open-circuit voltage.

There are several tools available to simulate PV modules under different environmental conditions. One of the most used tools is *pvlib*, a library providing a set of classes and methods for simulating PV systems [19]. *Pvlib* can simulate PV cells and modules under conditions of different illumination, which is demonstrated in this manuscript, but cannot generate I-V nor P-V characteristics of modules and series connection of modules that are partially shaded or soiled, nor can take into account the effects of safety bypass diodes in the calculation.

In order to eliminate these shortcomings, a set of classes was developed, which allow the generation of equivalent module characteristics. A detailed description of this software is given in [23]. Using this tool to simulate modules under non-uniform conditions, the characteristics shown in Fig. 10 were generated. This tool enables the generation of characteristics of more complex photovoltaic structures. Both simulated module characteristics, which are presented in this manuscript, and measured module characteristics can be used as input [22].

Acknowledgement: *This manuscript is a part of the research supported by Agreements 451-03-47/2023-01/200102 on the realization and financing of scientific research work of the Faculty of Electronic Engineering, University of Niš in 2024 by the Ministry of Science, Technological Development and Innovation of the Republic of Serbia.*

REFERENCES

1. Lindsey, R. and Dahlman, L. (2021) Climate Change: Global Temperature, https://www.climate.gov/news-features/understanding-climate/climate-change-global-temperature, (accessed 27.7.2024.)
2. Ocean & Climate Platform, (2024) Ocean acidification, https://ocean-climate.org/en/awareness/the-impact-of-climate-change-on-the-ocean/, (accessed 27.7.2024.)
3. Pelejero, Carles; Calvo, Eva; McCulloch, Malcolm T.; Marshall, John F.; Gagan, Michael K.; Lough, Janice M.; Opdyke, Bradley N. (2005). "Preindustrial to Modern Interdecadal Variability in Coral Reef pH". Science. 309 (5744), pp. 2204–2207, doi:10.1126/science.1113692.
4. European Environment Agency, Global and European sea level rise, https://www.eea.europa.eu/en/analysis/indicators/global-and-european-sea-level-rise (accessed 27.7.2024.)
5. Sattar Q, Maqbool ME, Ehsan R, Akhtar S (2021) Review on climate change and its effect on wildlife and ecosystem. Open J Environ Biol 6(1): 008-014. DOI: 10.17352/ojeb.000021
6. Attribution of Extreme Weather Events in the Context of Climate Change (Report). Washington, DC: The National Academies Press. 2016. pp. 21–24. doi:10.17226/21852. ISBN 978-0-309-38094-2.
7. International Energy Agency, Renewables 2023, Analysis and forecast to 2028, https://iea.blob.core.windows.net/assets/96d66a8b-d502-476b-ba94-54ffda84cf72/Renewables_2023.pdf
8. Residential Solar PV Systems Market, Global Outlook and Forecast 2023-2030, https://www.linkedin.com/pulse/residential-solar-pv-systems-market-global-outlook-oomrf
9. Eltawil, M. A., & Zhao, Z. (2013). MPPT techniques for photovoltaic applications. *Renewable and sustainable energy reviews*, *25*, 793-813.
10. Kamarzaman, N. A., & Tan, C. W. (2014). A comprehensive review of maximum power point tracking algorithms for photovoltaic systems. *Renewable and Sustainable Energy Reviews*, *37*, 585-598.
11. Verma, D., Nema, S., Shandilya, A. M., & Dash, S. K. (2016). Maximum power point tracking (MPPT) techniques: Recapitulation in solar photovoltaic systems. *Renewable and Sustainable Energy Reviews*, *54*, 1018-1034.
12. *Al-Ezzi, Athil S.; Ansari, Mohamed Nainar M. (8 July 2022). "Photovoltaic Solar Cells: A Review". Applied System Innovation.* ***5*** *(4): 67. doi:10.3390/asi5040067. ISSN 2571-5577.*
13. *"Photovoltaic... Cell, Module, String, Array". WordPower—Ian Woofenden. 2006. Archived from the original (PDF) on --August 19, 2016. Retrieved December 28, 2018.*
14. Andrejevic-Stosovic, M., Litovski, I., Lukac, D., Dimitrijevic, M., and Litovski, V. (2014). Small signal model of a solar cell. Simulation, Trans. of the Society for Modeling and Simulation, International, pages 1-14.
15. Andrejevic-Stosovic, M., Lukac, D., Litovski, I., and Litovski, V. (2012). Frequency domain characterization of a solar cell. In Proc. of the 11th Symp. on Neural Network Application in Electronic Engineering, NEUREL, pages 259-264.
16. Ćalasan M, Abdel Aleem SHE, Zobaa AF. On the root mean square error (RMSE) calculation for parameter estimation of photovoltaic models: A novel exact analytical solution based on Lambert W function. Energy Convers Manag 2020;210:112716. https://doi.org/10.1016/j.enconman.2020.112716.
17. Wolfram Mathworld, Lambert W-function, https://mathworld.wolfram.com/LambertW-Function.html
18. M. Tripathy, M. Kumar, P.K. Sadhu: Photovoltaic system using Lambert W function-based technique, Solar Energy, Volume 158, 2017, Pages 432-439, ISSN 0038-092X, DOI 10.1016/j.solener.2017.10.007.
19. PV Performance Modeling Collaborative | PV_LIB Toolbox n.d. https://pvpmc.sandia.gov/applications/pv_lib-toolbox/ (accessed March 12, 2023).
20. S. M. Ryvkin, (2014) *Physics of p-n Junctions and Semiconductor Devices*, Springer US.
21. A.J. Anderson, (1996), *Photovoltaic translation equations: A new approach*, Final subcontract report, doi: 10.2172/177401.
22. M. P. Petronijević, I. Radonjić, M. Dimitrijević, L. Pantić, M. Ćalasan, (2024), *Performance evaluation of single-stage photovoltaic inverters under soiling conditions*, Ain Shams Engineering Journal, Volume 15, Issue 1, doi:10.1016/j.asej.2023.102353.
23. M. A. Dimitrijević, M. Petronijević (2024), *Emulation of Photovoltaic Arrays Under Nonuniform Environmental Conditions*, 21st International IGTE Symposium 2024 on Computational Methods in Electromagnetics and Multiphysics, accepted for publication.

UTICAJ SIGURNOSNIH DIODA NA KARAKTERISTIKE FOTONAPONSKIH PANELA U NEUJEDNAČENIM UTICAJIMA SREDINE

Rad fotonaponskih sistema zavisi od uticaja sredine, koji utiču na strujno-naponske karakteristike fotonaponskih modula i složenijih struktura koje se realizuju njihovim povezivanjem. Pri neujednačenim uslovima sredine – različitim osvetljajem ćelija unutar jednog modula – karakteristike modula mogu biti kompleksne. Ovoj kompleksnosti doprinose i sigurnosne bajpas diode, koje su povezano paralelno ćelijama i štite ih od pregrevanja prilikom delimičnog zasenčenja. Kako bi se procenile performanse fotonaponskog sistema, konkretno invertera i algoritma za pronalaženje maksimalne snage, neophodno je uzeti u obzir ove uticaje na karakteristike fotonaponskih struktura. U ovom rukopisu će biti razmotren uticaj osvetljaja i temperature na pojedinačne fotonaponske ćelije, topologija fotonaponskog modula koja uključuje bajpas diode, kao i karakteristike modula sa zaštitnim bajpas diodama pri neujednačenim uticajima sredine.

Ključne reči: *fotonaponska ćelija, fotonaponski modul, bajpas diode, strujno-naponske karakteristike*

FACTA UNIVERSITATIS
Series: **Working and Living Environmental Protection** Vol. 21, Nº 2, 2024, pp. 133 - 141
https://doi.org/10.22190/FUWLEP240610012R

Review Paper

CONSTRUCTION, DEMOLITION, AND RENOVATION WASTE

UDC 628.477.6.036

Jasmina Radosavljević, Ana Vukadinović

University of Niš, Faculty of Occupational Safety, Niš, Serbia

ORCID iDs: Jasmina Radosavljević https://orcid.org/0000-0001-8545-2265
Ana Vukadinović https://orcid.org/0000-0002-6228-1077

Abstract. *Increased construction and demolition activities have led to a rise in construction and demolition waste. Construction waste is generated during the construction, adaptation, and demolition processes. Its quantities depend on the materials used, construction techniques, and types of projects. In Serbia, the management of such waste is regulated by specific legislation. This paper provides a classification of construction waste according to the European waste catalog and describes its generation, management, and the possibilities for estimating waste before the commencement of construction work. The possibilities and main obstacles to recycling this waste are also described.*

Key words: *C&D (construction and demolition) waste, C&D waste management plan, estimation of C&D waste quantities, C&D waste recycling*

1. INTRODUCTION

The problem of waste generation, including waste from construction, renovation, and demolition of buildings, is a global issue. Construction waste encompasses all waste generated as a result of demolition, construction, and renovation activities in Europe, accounting for 25-30% of total generated waste. Accordingly, the construction industry significantly contributes to environmental degradation and the consumption and depletion of natural resources [1-2].

- Construction waste is generated as a result of works carried out on buildings from the foundation upwards, as well as civil engineering works such as the construction of roads, railways, canals, dams, sports and recreation facilities, ports, airports, and the like. The composition of construction waste depends on the type of construction work and the techniques used. Construction waste is classified based on its content

Received June 10, 2024 / Accepted October 11, 2024
Corresponding author: Ana Vukadinović
Faculty of Occupational Safety, Čarnojevića 10a, 18000 Niš, Serbia
E-mail: ana.vukadinovic@znrfak.ni.ac.rs

and composition according to the European waste catalog. It is divided into five main categories:

- Soil (sand, clay, stones, mud, etc.) is generated from pre-construction excavations. This waste can be mixed with organic plant elements.
- Packaging waste from construction materials (wooden pallets, plastic, cardboard, etc.) that are less prevalent in construction works.
- Residual construction materials (natural stone: concrete, ceramics, aggregates and their mixtures; non-stone: steel, iron, aluminum, copper, glass, wood, plastic, asphalt, etc.), which are more homogeneous in construction works.
- Hazardous waste (contaminated soil and excavations, materials and substances with potentially hazardous characteristics: flammable concrete additives, adhesives (flammable, toxic, or irritating), tar emulsions (toxic, carcinogenic), asbestos-based materials in breathable fiber form (toxic, carcinogenic), wood treated with fungicides, pesticides, etc. (toxic, ecotoxic, flammable), coatings with halogenated flame retardants (ecotoxic, toxic, carcinogenic), equipment with PCBs (ecotoxic, carcinogenic), mercury lighting (toxic, ecotoxic), systems with CFCs, gypsum components (possible sources of sulfides in landfills, toxic, flammable), containers for hazardous substances (solvents, paints, adhesives, etc.), and contaminated waste packaging.
- Other (organic materials) [3-4].

Construction waste can be generated due to:

- Material losses during transport to the construction site, unloading, and initial storage.
- Improper storage of materials leads to material loss due to exposure to rain and/or pedestrian/vehicle traffic.
- Cutting of materials into different sizes and uneconomical shapes.
- Improper enclosure of remaining materials in containers and metal boxes, causing hardening of excess materials left after use.
- Damage caused by subsequent works.
- Theft and vandalism.
- Lack of supervision or incorrect management decisions.
- Improper use or incorrect selection of materials.

Construction and demolition (C&D) waste constitutes more than one-third of the total waste generated in the European Union. In recent years, there has been a construction boom in Serbia, increasing the demand for construction materials. Additionally, the amount of demolition waste has increased. Increased construction and demolition activities have led to a rise in C&D waste. Large quantities of construction waste end up in landfills, by roadsides, and in nature. However, large portions of this waste can be reused. According to estimates, around 3 to 4 million tonnes of construction waste are generated annually in Serbia, not only from demolition and construction but also from major infrastructure works, such as road and railway construction, as well as works like water and sewage construction, resulting in a significant amount of waste.

Materials such as concrete, bricks, wood, glass, metals, and plastics, essentially all waste generated from the construction and demolition of structures and infrastructure, as well as from planning and maintenance of roads, end up in landfills. Through recycling, all of this waste can be reused, thereby preserving resources and protecting the environment. In some European countries, like the Netherlands and Denmark, up to 90%

of the total amount of construction waste is recycled. This type of waste is a national resource that should be utilized, and the first steps in solving the problem of construction waste management involve amending the relevant legislation.

The Government of the Republic of Serbia adopted the Regulation on the Manner and Procedure for Construction and Demolition Waste Management, which for the first time stipulates how this waste should be managed. The goal of the Regulation is to prevent the creation of illegal landfills and to allow the waste to be used in construction. The aim of the Regulation is to change habits, existing practices, and rules so that construction waste in this case becomes a resource.

Among other things, the amount of construction waste can be reduced through proper management of waste materials on construction sites. Investors are legally required to develop a Construction and Demolition Waste Management Plan.

2. Construction and Demolition Waste Management Plan

Construction waste is generated from construction and other works related to building construction and demolition, adaptation, renovation, and reconstruction; construction, maintenance, and replacement of infrastructure facilities; excavations for residential, industrial, and road infrastructure construction; and demolition of built structures.

The management of construction waste involves a set of activities and measures that include separate collection, sorting, transport, storage, preparation for reuse, recycling, and/or disposal of construction waste.

Measures for C&D waste management include:

- Extracting useful components from and within the building before starting construction and other works, which are not considered waste according to the law regulating waste management and which can be reused for the same purpose for which they were produced (bricks, tiles, etc.).
- Preventing the mixing of hazardous and non-hazardous C&D waste and the mixing of different types of waste.
- Preventing the dispersal, spillage, and leakage of hazardous waste into the soil, surface and groundwater, and air.
- Determining the location for temporary storage of C&D waste at the site of generation, i.e., at the construction site.
- Testing and classifying C&D waste.
- Carrying out works in a way that prevents waste generation.
- Encouraging the reuse and recycling of C&D waste.
- Keeping records and reporting on the quantity and type of generated C&D waste, as well as the treatment it has undergone [5].

C&D waste should be separated at the site of generation to prepare it for treatment, i.e., reuse, including processes like backfilling and disposal. Uncontrolled disposal of such waste is prohibited.

Figure 1 shows the demolition works.

Fig.1 Demolition works. [6]

According to the Law on Waste Management, Article 58a ("Official Gazette of the RS", No. 36/2009, 88/2010, 14/2016, 95/18 – other law, and 35/2023), which stipulates the management of C&D waste, and according to the Regulation on the Manner and Procedure for Construction and Demolition Waste Management ("Official Gazette of the RS", No. 93/2023 and 94/2023 – corrected), a C&D Waste Management Plan is developed and is part of the documentation submitted with the application for obtaining a construction permit. According to Article 6 of the Regulation on the Manner and Procedure for Construction and Demolition Waste Management ("Official Gazette of the RS", No. 93/2023), the producer of C&D waste (the investor, the owner of the C&D waste) is required to develop a C&D Waste Management Plan, obtain approval for the Plan, and organize its implementation if the works are carried out on a category B, V, and G building according to the Rulebook on Classification of Buildings ("Official Gazette of the RS", No. 22/2015). The approval decision for the C&D Waste Management Plan is submitted along with the application for the construction permit or the decision on approval for construction.

The C&D Waste Management Plan contains information on:

- The type and planned quantity of waste that will be generated by activities on the construction site during construction, demolition, adaptation, reconstruction, and other works on a building or part of a building.
- The location of containers for collecting C&D waste.
- The method of separate waste collection, preparation for transport, and temporary storage of the waste in question.
- Handling of hazardous waste that is expected to be generated during the execution of works.
- Methods for reusing C&D waste.
- The quantity and type of C&D waste planned to be handed over to an operator of a facility for the reuse of waste, i.e., planned quantities sent for processing/recycling.
- The intended methods for C&D waste treatment.
- The estimated volume of soil excavation, resulting from construction works on the site, and its handling [5, 7, 8].

3. Estimation of the Quantity of Construction Waste Generated at Construction Sites

The types and quantities of waste generated at construction sites depend on the characteristics of the materials used and the construction techniques employed during the construction process. Thus, the waste will vary depending on the project. There are generally two procedures for estimating the quantities of waste generated:

- Quantification procedure for obtaining approximate estimates using waste quantification tables.
- Quantification procedure for obtaining specific estimates for each project.

The methodology for such cases is as follows:

- Step 1: Obtaining waste quantification tables classified by type of project (demolition, construction, renovation); purpose (residential, nonresidential: industrial, commercial, etc.); and relevant technologies for the project (prefabricated construction, masonry, etc.).
- Step 2: Identifying the characteristics of the project: type of project (demolition, construction, renovation); purpose (residential, nonresidential: industrial, commercial, etc.); and main technologies (usually construction-related: metal, concrete, or masonry).
- Step 3: Calculating the project area (in m^2).
- Step 4: Obtaining the total quantity of waste (volume and/or weight) from the floor area of the project.
- Step 5: Determining the composition of the waste (quantities by type of waste) [9].

Waste quantification tables (Tables 1 and 2) can be used to obtain approximate data on C&D waste.

Table 1 Weighted average C&D (construction and demolition) waste generation rates (kg/m^2) [9]

Type of construction	Heavyweight construction: masonry, concrete, etc.		Lightweight construction: precast elements, drywalls, wood frame, etc.	
Type of building	Residential building	Nonresidential building	Residential building	Nonresidential building
New building construction	120-140	100-120	20-22	18-20
Rehabilitation	300-400	250-350	90-120	80-90
Demolition	800-1000	500-700	500-700	700-800

Table 2 Volume average C&D (construction and demolition) waste generation rates (m^3/m^2) [9]

Type of construction	Heavyweight construction: masonry, concrete, etc.		Lightweight construction: precast elements, drywalls, wood frame, etc.	
Type of construction	Residential building	Nonresidential building	Residential building	Nonresidential building
New building construction	0.12-0.14	0.10-0.12	0.02-0.03	0.02-0.03
Rehabilitation	0.30-0.40	0.25-0.35	0.10-0.15	0.09-0.10
Demolition	0.80-1.00	1.00-1.20	0.50-0.70	0.70-0.08

Table 3 shows the average composition of construction waste by volume in construction.

Table 3 Rounded average percentage of waste composition by volume in constructions (%) [9]

Type of waste	Heavyweight construction: masonry, concrete, etc. (%)	Lightweight construction: precast elements, drywalls, light frame, etc. (%)
15 Packaging waste	60-70	30-60
15 01 01 Paper cardboard pack	2-4	1-4
15 01 02 Plastic packaging	5-7	2-3
15 01 03 Wooden packaging	50-55 and 17 02 01wood*	25-45
15 01 04 Metallic packaging*	2-3 and 17 04 metals	2-7
15 01 06 Mixed packaging	< 1	< 1
17 C&D waste	30-40	40-70
17 01 01 Concrete	15-20	10-30
17 01 03 Ceramics-bricks	10-13	-
17 01 07 Mixed concrete, ceramics	2-3	-
17 08 02 Drywalls	-	20-25
17 09 04 Mixed C&D waste	3-4	10-15
17 05 Soil and stones	Varies	Varies

Table 4 Rounded average percentage of waste composition by volume in demolitions (%) [9]

	Residential		Nonresidential	
Type of waste	Masonry (%)	Concrete (%)	Metal (%)	Concrete (%)
17 01 01 Concrete	5-10	40-50	15-20	35-40
17 01 03 Ceramics-blocks mixtures	65-70	20-30	15-20	5-10
17 01 07 Concrete-ceramics	5-10	5-10	35-40	40-45
17 02 01 Wood	1-5	1-5	0.3	0.2
17 02 02 Glass	0.1	0.1	0.2	0.1
17 02 03 Plastics	0.1	0.1	0.8	0.8
17 02 03 Asphalt	0.5	0.5	0.1	4
17 04 01/05 Metals	1-2	2-3	10-15	1-5
Potentially hazardous*	2-10	2-10	0.6	0.2
17 09 04 Mixed C&D waste			5-10	5-10

Table 5 Rounded average percentage of waste composition by volume in rehabilitations (%) [9]

Type of waste	Heavyweight construction: masonry, concrete, etc.	Lightweight construction: precast elements, drywalls, light frame, etc.
15 Packaging waste	35-70	30-70
15 01 01 Paper cardboard pack	1-6	2-4
15 01 02 Plastic packaging	3-8	2-5
15 01 03 Wooden packaging	25-45	20-40
15 01 04 Metallic packaging*	5-15	5-20
15 01 06 Mixed packaging	< 1	< 1
17 C&D waste	25-65	30-70
17 01 01 Concrete	5-10	5-10
17 01 03 Ceramics-bricks	5-15	
17 01 07 Mixed concrete ceramics	10-25	
17 08 02 Drywalls		20-35
17 09 04 Mixed C&D waste	5-15	5-25
17 05 Soil and stones	Varies	Varies

*Waste fulfils at least one criterion for danger.

The data provided in Tables 1-5 can be useful for waste planning and management during construction, demolition, and renovation, allowing a more precise estimation of resources and more efficient waste management.

4. Construction Waste Recycling

As a consequence of intensified construction in Serbia, large quantities of construction waste are generated through activities such as demolition, construction, renovation, adaptation, and other technical maintenance. The increase in these activities has not been matched by the necessary infrastructure for the reception and disposal of construction waste, leading to issues in managing this type of waste and often resulting in illegal dumping at inadequate locations. Handling this waste stream requires a specific approach. The practice of uncontrolled dumping of C&D waste should be abolished as soon as possible. Owners of construction waste should be responsible for the costs of C&D waste management and are required to ensure separate collection and temporary storage.

Currently, there is no practice of separate collection of C&D waste, nor is there a recycling scheme for this type of waste. Construction waste has a very high potential for recycling and is recognized at the European level as a priority waste stream.

Although there is a general legal obligation for the waste producer to collect the generated waste separately and sort it according to future treatment processes in the amount, i.e., percentage, according to the national goals (Article 26 of the Law on Waste Management), this provision does not apply to C&D waste. Typically, only high-value recyclable waste, such as metal, is recycled, while other potentially recyclable materials are disposed of in landfills or, more often, at unsecured local dumpsites.

The following are the main obstacles to recycling construction and demolition waste:

- Legal uncertainty regarding the status of recycled C&D waste (there are still no regulations on the cessation of waste status except for glass, iron and steel, copper, and aluminum).
- Lack of thorough records of sources, quantities, and flows of construction waste, despite the existence of a legal framework, which is not enforced.
- Extremely large quantities of construction waste.
- Uncontrolled disposal of large quantities of construction waste.
- Absence of a system for separating construction waste at the source.
- No separation of hazardous construction waste.
- Lack of incentives for using recycled construction materials.
- No legal obligation for the waste producer to recycle this type of waste (even though the Law on Waste Management defines C&D waste as a priority waste stream for recycling).
- Lack of economic incentives, as mineral C&D waste can be disposed of at a relatively low cost.
- Lack of quality standards for recycled C&D waste (especially in terms of environmental performance), causing liability issues.
- The issue of construction waste is often neglected during the design phase of projects and is not sufficiently regulated by by-laws.
- Absence of a quality market for construction waste.
- Lack of effective communication between all participants in the construction waste management process [10].

5. Conclusion

At the end of a building's life cycle, the generated waste will predominantly depend on its type (residential, industrial), the deconstruction criteria adopted in the project (e.g., dry anchoring systems), construction procedures, and materials used in the building's construction (concrete, wood, or metal structure), and the demolition techniques that were used (selective dismantling versus traditional demolition). During the construction and adaptation of buildings, the types and amounts of waste generated on-site depend on the project type, the characteristics of the materials used, and the construction techniques employed.

The investor/contractor is required to handle construction and demolition waste in accordance with the Law on Waste Management and the Regulation on the Manner and Procedure for Construction and Demolition Waste Management, to possess the necessary documentation, to establish separate collection and temporary storage of the waste generated at the construction site, as well as to separate hazardous from non-hazardous construction and demolition waste on-site.

The reuse of waste material and recycling of construction waste has enormous potential because, in addition to saving resources and raw materials, it also allows for additional savings in terms of material costs, transport, and machinery.

To establish a successful and efficient waste management system, it is necessary to do the following: keep a record of the quantities of construction and demolition waste, which needs to be constantly updated; regularly update the Construction Site Register (biannually); establish a system for separating construction and demolition waste on-site; ensure separation of construction and demolition waste on-site by components to provide high-quality recycling material; ensure separation of hazardous construction and demolition waste on-site; build the necessary infrastructure for construction and demolition waste management (build recycling yards and transfer stations, set up mobile plants for the treatment of such waste); utilize construction and demolition waste (use excavated soil to backfill and level the terrain and devastated locations, recycle non-hazardous construction and demolition waste in the recycling yard); and improve inspection and supervision in order to control construction and demolition waste disposal at inadequate locations.

Acknowledgement: *This paper is a part of the research supported by the Ministry of Education, Science and Technological Development of the Republic of Serbia according to agreement No. 451-03-66/2024-03/ 200148.*

References

1. Rocío Quiñones, Carmen Llatas, Maria Victoria Montes and Isidro Cortés: Quantification of Construction Waste in Early Design Stages Using Bim-Based Tool, Recycling, 7, 63, 2022.
2. AET Group Inc., Construction, Renovation, and Demolition Waste Management Guidebook, December 12, 2023.
3. Agencija za zaštitu životne sredine, KATALOG OTPADA - Uputstvo za određivanje indeksnog broja [WASTE CATALOG – Instructions for determining index number], Beograd, 2010.
4. Rouhi Broujeni, Omrani, G.A., Naghavi, R., Afraseyabi S.S., Construction and Demolation Waste Management, Journal of Solid Waste Technology & Management.Vol. 6 (6): pp.1249–1252.
5. Regulation on the Manner and Procedure for Construction and Demolition Waste Management ("Official Gazette of the RS", No. 93/2023 and 94/2023 – corrected).
6. Mercedes del Rio Merino, Pilar Cristina Izquierdo, Isabel Salto Weis: Sustainable construction: construction and demolition waste reconsidered, Waste Manag Res., Vol. 28(2): pp.118-29, 2010.

7. Law on Waste Management ("Official Gazette of the RS", No. 36/2009, 88/2010, 14/2016, 95/18 – other law, and 35/2023).
8. Tom Napier, Construction Waste Management, Construction Engineering Research Laboratory (CERL), 2016, https://www.wbdg.org/resources/construction-waste-management.
9. C. LLATAS: Methods for estimating construction and demolition (C&D) waste, Woodhead Publishing Limited, 2013.
10. Mazen, M.Omer, Rahimi A. Rahman, Saud Almutairi, Construction waste recycling: Enhancement

GRAĐEVINSKI OTPAD OD GRAĐENJA, RUŠENJA I REKONSTRUKCIJE

Povećana izgradnja i rušenje objekata uslovile su porast građevinskog otpada od građenja i rušenja. Građevinski otpad se generiše prilikom izgradnje, adaptacije i rušenja otpada. Njegove količine zavise od upotrebljenih materijala, tehnike građenja i vrste projekata. U Republici Srbiji, upravljanje ovim otpadom regulisano je određenom zakonskom regulativom. U radu je data klasifikacija građevinskog otpada prema evropskom katalogu otpada, njegovo nastajanje, upravljanje ovim otpadom, mogućnosti procene otpada pre početka građevinskih radova. Takođe je opisana mogućnost i glavne prepreke reciklaže ovog otpada.

Ključne reči: *građevinski otpad (od gradnje i rušenja), plan upravljanja građevinskim otpadom, procena količine građevinskog otpada, reciklaža građevinskog otpada.*

CIP - Каталогизација у публикацији
Народна библиотека Србије, Београд

502/504

FACTA Universitatis. Series, Working and Living Environmental Protection / editor in chief Nenad Živković. - [Štampano izd.]. - Vol. 1, no. 1 (1996)- . - Niš : University of Niš, 1996- (Niš : Atlantis). - 24 cm

Dostupno i na:
http://casopisi.junis.ni.ac.rs/index.php/FUWorkLivEnvProt. - Tri puta godišnje. - Drugo izdanje na drugom medijumu: Facta Universitatis. Series: Working and Living Environmental Protection (Online) = ISSN 2406-0534
ISSN 0354-804X = Facta Universitatis. Series: Working and Living Environmental Protection
COBISS.SR-ID 72210956